Session IV

RESPONSE AND RESILIENCE OF CRYSTALLINE ROCK TO NATURAL PERTURBATIONS AND GEOSPHERE EVOLUTION (BUFFERING)

FRACTURE REACTIVATION IN RESPONSE TO SEISMIC EVENTS

H. Hökmark[1], B. Fälth[1], R. Munier[2]
[1]Clay Technology AB,
[2]Swedish Nuclear Fuel and Waste Management Company; Sweden

Abstract

The present paper describes a method to calculate fracture shear displacements occurring as a result of the stress waves and the static stress redistribution following a seismic slip on a nearby fault. Such secondary fracture shear displacements can theoretically, if large enough, damage intersected canisters containing spent nuclear fuel. The method is applied to a type of seismic event that is, or may be, of concern for the long term safety of a KBS-3 nuclear fuel repository: namely, endglacial earthquakes of magnitude 6 and larger. The numerical scheme used to simulate rupture initiation and propagation is described and illustrated. Result examples are given that show that secondary shear displacements on 300 m diameter fractures will be smaller than the damage criterion now applied by the Swedish Nuclear Fuel and Waste Management Co (SKB), provided that the fracture center is at a distance of 200 m or larger from the fault plane. The relevance of the rupture representation is discussed based on comparison with slip velocity records from a recent, large and well-documented crustal earthquake and with stress drop estimates made for large endglacial faults observed in Lapland, northern Sweden.

Introduction

In the Swedish KBS-3 concept for geological disposal of spent nuclear fuel, copper canisters with a cast iron insert containing the fuel are surrounded by bentonite clay for isolation and mechanical protection (SKB, 2006a). The canisters are deposited in vertical deposition holes in the floor of horizontal tunnels at between 400 and 700 m depth in crystalline rock (Figure 1, left). Large shear displacements along a rock fracture that intersects a canister could obviously damage the canister (Figure 1, right) in particular if the fracture shear velocity is high. Numerical analyses of the canister-buffer system have shown that shear displacements smaller than 0.1 m will give only modest plastic deformations in the iron insert and in the copper shell, even assuming unfavorable intersection geometries and high shear velocities (Börgesson and Hernelind, 2006).

In the SR-Can safety assessment, canisters sheared 0.1 m or more count as failed, irrespective of the canister-fracture intersection geometry and the fracture shear velocity (SKB, 2006a). Shear displacements of that magnitude cannot occur on fractures of extensions smaller than about 700 m for the predicted time-continuous reference load evolution of a KBS-3 repository at any of the SKB candidate sites, even assuming low shear strength and worst case orientation of the intersecting fracture (Hakami and Olofsson, 2002; Hökmark *et al.,* 2006). Since fractures of that size or larger will be detected during the repository construction (see following sections), it will be possible to reject positions where canisters could be exposed to the risk of direct damage due to fracture shear displacements caused by time-continuous load changes, for instance during the period of thermal load

following closure, or during periods of glaciation. There are, however, uncertainties regarding the risks of seismic events occurring reasonably close to the site selected for the repository as well as the consequences of such an event.

Figure1. **Fracture Shear Displacement across KBS-3 Canister**

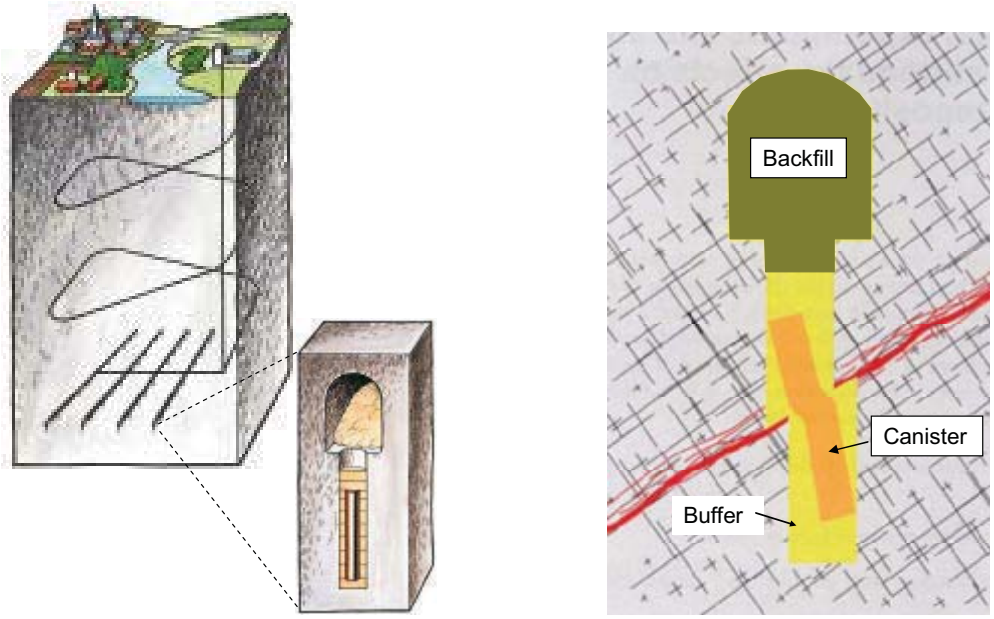

Present-day Sweden is a low seismicity area with most earthquakes being observed in the south-west, along the north-east coast and in Norrbotten. The area in the south-east, where SKB's candidate sites Forsmark and Laxemar are located, is relatively inactive. Although large earthquakes (magnitude about 8) have occurred in Sweden, it is generally agreed that these were connected to the late stages of deglaciation at the end of the previous ice-age (Lagerbäck, 1988; Arvidsson, 1993; Bödvarsson *et al*., 2006). While all unambiguous traces of such large endglacial earthquakes appear to be located in northern Scandinavia where the ice-cap was thickest and had the longest unbroken duration, it cannot be excluded that some may have occurred also in central and southern Sweden (Munier and Hökmark, 2004). This means that there may be a non-zero risk of large earthquakes occurring close to the potential repository sites in connection with the disappearance of future ice-covers, and that the probability of canisters being damaged, for instance as shown in Figure 1 (right), must be assessed.

Shear displacements and canister damage

Slip on earthquake faults

Figure 2(left) shows correlations between moment magnitude and surface displacement derived by Wells and Coppersmith (1994) from a database of 224 well-documented crustal earthquakes. A fault displacement of 0.1 m, which corresponds to the SR-Can canister damage threshold for fractures intersecting canisters, appears to require an earthquake of moment magnitude 5 or larger. Figure 2 (right), which gives corresponding relations between magnitude and rupture area, shows that a magnitude 5 earthquake requires a rupture area of between 2 km^2 and 30 km^2. Both plots are redrawn from Wells and Coppersmith (1994).

Figure 2. **Moment magnitude as function of maximum earthquake slip and rupture area**

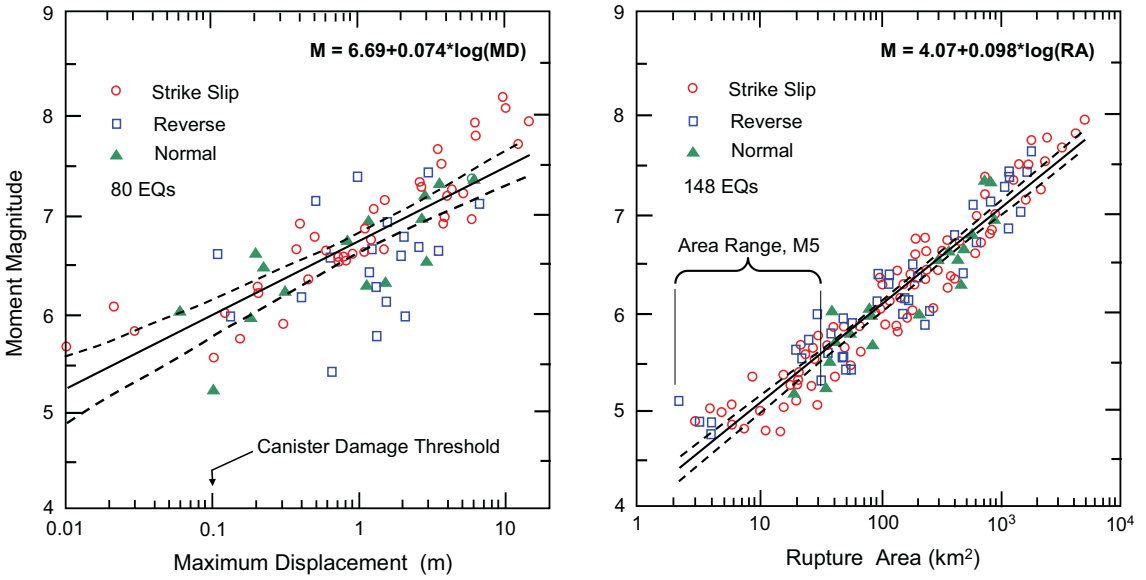

Figure 3 gives direct size-displacement relations, size being represented by the surface rupture length and displacement by the maximum (left) and average (right) fault slip at the ground surface. Both plots are redrawn from Wells and Coppersmith (1994). Provided that the regressions are valid for small events and that the surface displacement is a reasonably relevant measure of the subsurface fault slip at shallow depths such as the repository depth, the plots suggest that seismic events on faults smaller than about 2 km are not likely to give any canister damage.

Figure 3. **Maximum displacement and average displacement as function of surface rupture length**

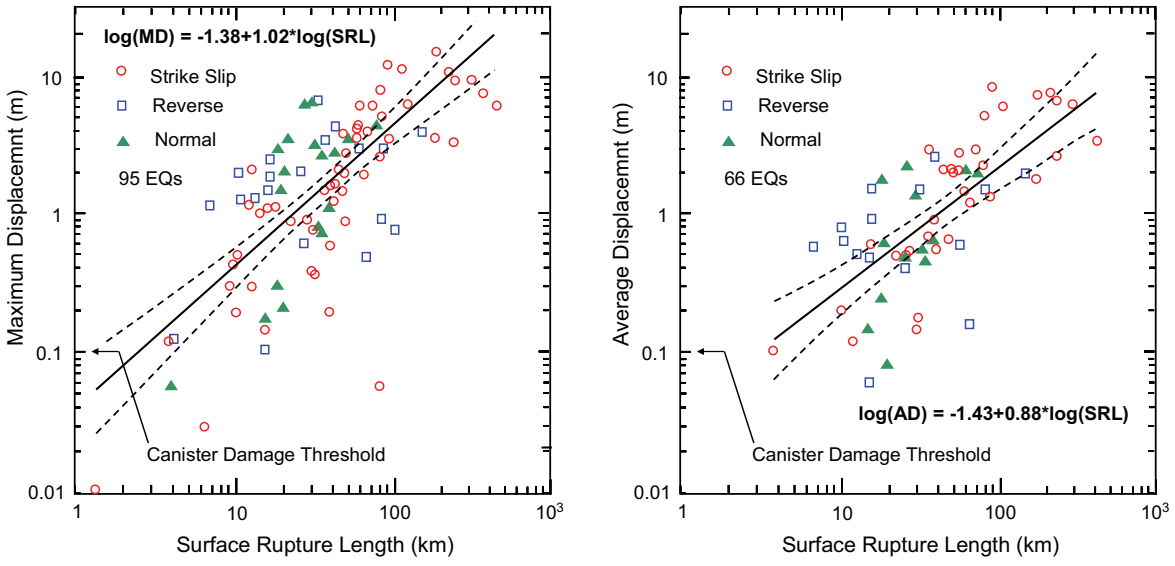

The regressions in Figure 3 are based mainly on records of magnitude 6 events and larger, with few records of events smaller than magnitude 5. (La Pointe *et al.,* 1997) discuss the relevance of the regressions for small events and mention that Slunga (1991) reported that the magnitude 4.5 Skövde

earthquake hade a peak displacement of about 300 mm. The focal depth of the Skövde event was, however, about 26 km, i.e. far below the typical repository depth.

Very few canisters would be intersected by kilometer-sized fractures at any of the SKB candidate sites even if all deposition holes were positioned blindly according to the reference layout, i.e. without any attempts to detect and avoid large fractures. Applying detection criteria defined by Munier (2006) reduces the number of intersected deposition holes further as shown in Figure 4: Out of the 6 000 canisters planned to be deposited within the Swedish programme, not more than two in Forsmark and one in Laxemar would be intersected by fractures larger than 300 m in diameter. For comparison the size-displacement regressions (see Figure 3) are shown along with the size-intersection relations. The extrapolated curves indicate that fractures larger than about 600 m should be safely detected. In conclusion, potential earthquake faults appear to be (with a good margin) either too small to give a fault slip of 0.1 m or more, or too large to avoid detection during construction. This means that slip on earthquake faults cannot be expected to damage any canisters.

Figure 4. **Number of canisters intersected vs. fracture size**

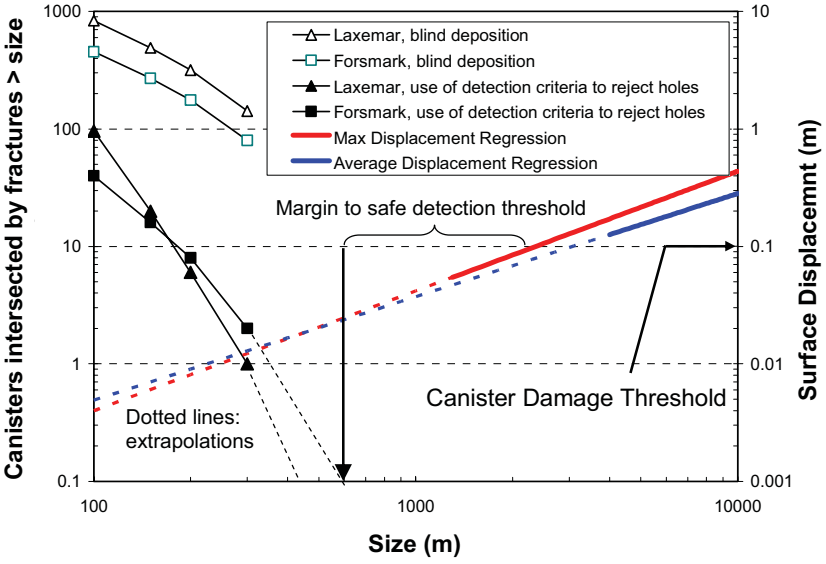

Secondary displacements

Large earthquakes occurring at some distance from the canisters may induce shear displacements on nearby fractures which, in turn, may intersect canister positions. Such secondary, induced, fracture shear displacements will occur immediately in direct response to the stress waves and the redistribution of the static stresses following rupture and slip on the primary fault on which the earthquake originates. Together with the in-situ stresses, the dynamic and static stress additions may exceed the stability margin of individual nearby fractures significantly, meaning that displacements may, at least theoretically, be considerable also on fractures just a few hundred meters in diameter.

Aftershocks that take place on nearby faults or neighboring fault segments with a time delay of minutes, hours or days are a process of relaxing stress concentrations produced by the rupture of the mainshock (Scholz, 2002). There does not seem to be any reason to believe that size-displacement correlations for aftershocks should be essentially different from those shown for mainshocks in Figure 3. This means that both types will occur on features that are either to small to give a 0.1 m displacement or too large to avoid detection during construction. For the purpose of this study there is

no reason to distinguish between mainshocks and aftershocks (or foreshocks), i.e. both may theoretically induce secondary displacements on nearby fractures,

Studies of secondary shear displacements and their potential to damage canisters in the KBS-3 repository have been reported previously by La Pointe *et al.* (1997), La Pointe *et al.* (1999) and Munier and Hökmark (2004). The previous work was based on idealized descriptions of the rupture process and the properties of the rock fractures, leading to overly conservative estimates of the resulting secondary displacements. The results described and discussed here are based on work reported by Fälth and Hökmark (2006) and work in progress (Fälth and Hökmark, 2007).

Problem statement

The seismic concern that appears to be most relevant to the long term safety of the KBS-3 repository is the possibility of secondary displacements induced at repository depth by seismic dip-slip events on steeply dipping reverse type faults (i.e. similar to the endglacial earthquakes reported to have occurred in northern Fennoscandia some 10 000 years ago).

The objective now is to establish, using more elaborate numerical models than those tried in previous work, whether or not large fractures, yet smaller than the safe detection threshold (cf. Figure 4), and with different orientations will slip by more than the 0.1 m damage threshold if subjected to the dynamic and static stress effects of endglacial type events with moment magnitudes in the range 6.0 – 7.5, occurring at distances in the range 200 m – 1 000 m. The moment magnitude Mw is given by:

$$M_w = 0.667 \cdot \log_{10} M_0 - 6.07, \quad (1)$$

$$M_0 = \mu \cdot \bar{u} \cdot A \quad (2)$$

(M_0 = seismic moment, μ =shear modulus, $\bar{u}$ = average fault shear displacement, A = rupture area)

Numerical Approach

Model outlines

The analyses described below were performed using the three-dimensional distinct element code 3DEC, developed specifically to model mechanical and thermo-mechanical process in media containing numerous intersecting discontinuities such as rock fractures (Itasca, 2003). The code has logic for both static and dynamic analyses. In order to propagate stress waves properly, dynamic 3DEC analyses require finely meshed models, with zone edge lengths not larger than one eighth of the wavelength associated with the highest frequency considered. This means that events larger than magnitude 6 cannot be modeled using present-day computational capabilities (Fälth and Hökmark, 2006). However, it is possible to model a thick slice of a rock volume intersected by a fault large enough to host a magnitude 7 or magnitude 8 earthquake, although the truncated models will not be able to capture the response around the fault edges and not give fully accurate results a few seconds after rupture initiation when irrelevant reflections in the truncation plane begin to influence (Fälth and Hökmark, 2007). Figure 5 (left) shows outlines of a full magnitude 6 model and a truncated magnitude 7.5 model. Figure 5 (right) illustrates the mesh density and the mesh density variation of a 3DEC magnitude 6 model. The dimensions of the primary faults were specified to give rupture areas large enough to host earthquakes of the intended magnitudes. The fault dip angle was set at 70º for all models described here.

Figure 5. **Outlines of 3DEC models**

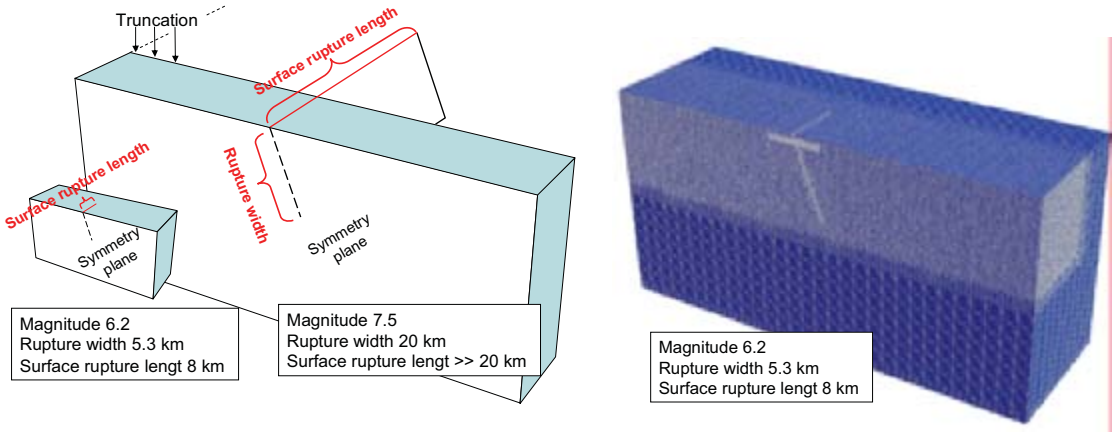

Target fractures

A number of 300 m diameter fractures, "target fractures", were located at 500 m depth and at different distances from the primary fault. Figure shows this for a magnitude 6 case. The left part shows the block structure of the 3DEC model. Note that the orthogonal cuts are construction planes, not fractures. The target fractures are located within the 100 m slice denoted "repository region". The right part shows a plane view of that region, with circles representing individual 300 m diameter perfectly planar target fractures of different orientations. In this particular model, the target fractures are either horizontal or dip 45º with dip directions 90º (same as fault) or 270º. In other models dip directions 45º, 135º, 225º and 315º were tried.

Values of target fracture stiffness and strength parameters were set according to the rock fracture description provided in the Forsmark and Laxemar site models (SKB, 2005; SKB, 2006b).

Figure 6. **Target fractures in the repository region**

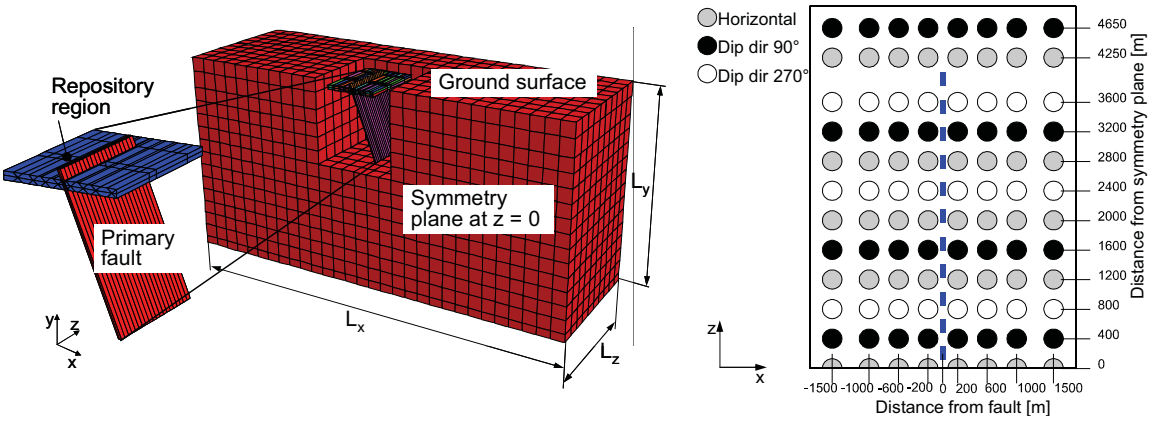

Initial and boundary conditions

In situ stress and pore pressure

Postglacial, or endglacial, stress states are characterised by high horizontal stresses which are due to downwarping and/or tectonic strain accumulated under the stabilizing ice cover, whereas the

vertical stress corresponds to the rock overburden. Here, the major initial horizontal stress was oriented normally to the fault strike and calibrated to give the average fault displacement needed to obtain the intended seismic moment, assuming that the fault shear strength has effectively dropped to zero after the rupture. For the geometry assumed here the minor horizontal stress is not important to the fault behavior (whereas it may be for target fractures). The horizontal and vertical stress components were taken to be principal stresses. Figure 7 (left) shows the stresses as function of depth as assumed in the magnitude 6 models. The Mohr circle plot in Figure 7 (right) illustrates the general stability conditions for target fractures at repository depth, with specifically indicated stability margins for horizontal fractures and fractures dipping 45º along the major horizontal stress. Points on the semicircles correspond to stress states in the principal stress planes, while points in the shaded area correspond to states in arbitrarily oriented planes. Here the effects of a 5 MPa pore pressure are included. The pore pressure influences the stability of the target fractures, but not the programmed behavior of the earthquake fault (see following sections).

Figure 7. ***In Situ* stress field assumed in magnitude 6 models**

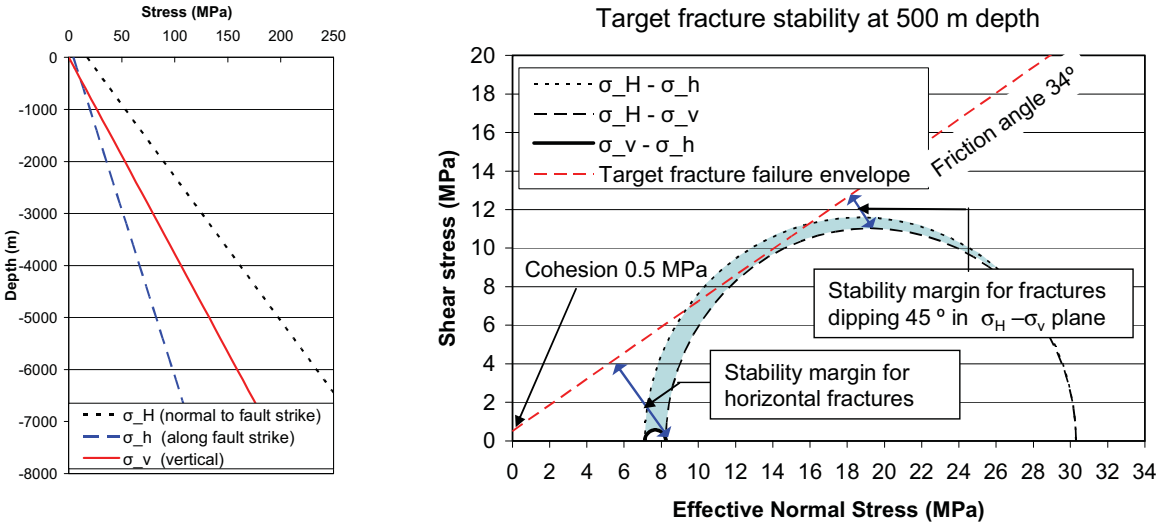

Fault shear strength

The fault cohesion was set just high enough to prevent failure before rupture, and then ramped down to initiate and control the rupture as described below. The residual fault shear strength was arbitrarily set to zero.

Boundary conditions

All boundaries with exception of the top boundary, which was free to allow for surface reflections, the symmetry plane and the truncation plane (magnitude 7.5 only, cf. Figure) which were locked in the normal direction, were viscous, i.e. non-reflecting.

Rupture initiation and propagation

The 3DEC code contains a built-in programming language, FISH, which was used here to initiate the rupture at the selected hypocenter and to propagate the rupture outwardly along the plane of the fault with a speed corresponding to 70% of the shear wave velocity of the surrounding elastic medium.

Figure 8 illustrates this for one of the magnitude 6 cases. The left part shows how the fault shear stress varies with time at four points, located at hypocenter depth at different horizontal distances from the hypocenter. When the rupture front arrives, the shear strength is ramped down to zero over a specified period of time, e.g. 0.5 seconds. The right part shows corresponding fault shear displacement at those points.

Figure 8. **Fault Shear Stress and Fault Slip as Function of Time – Magnitude 6**

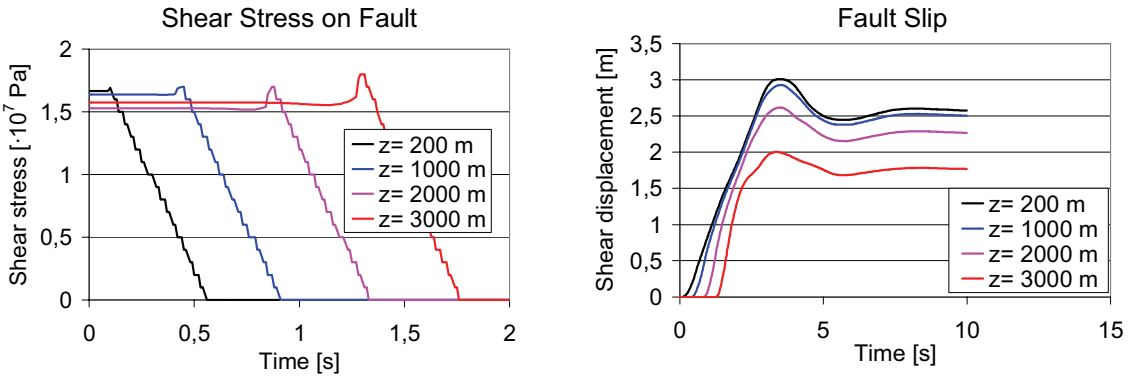

The vector plots in Figure 9 show the fault slip at three different instances of time. At the end of the process the average displacement is about 1.9 m and the maximum 3 m (at ground surface).

Figure 9. **Fault Shear Displacement Vectors at Different Times - Magnitude 6**

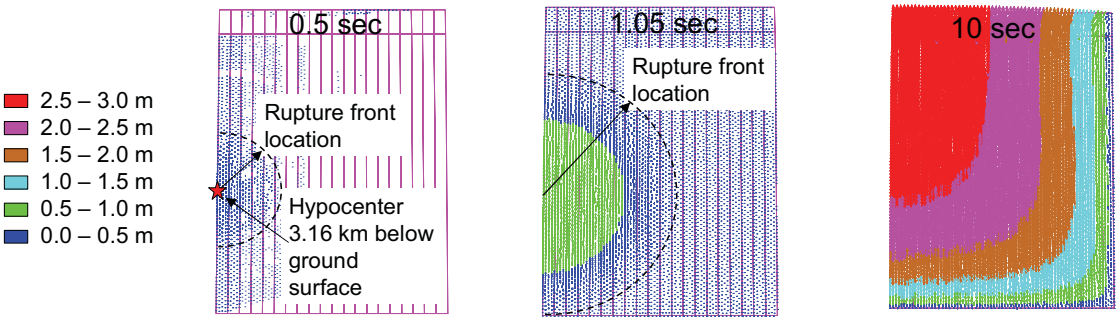

Results

Magnitude 6 events

Figure 10 shows induced shear displacement as function of time for target fractures dipping 45º and striking 180º relative to the fault (i.e. dip direction 270º, cf. Figure 6). The fractures with the largest peak displacements on the footwall and hanging wall sides were selected for this plot. Similar results, i.e. with a very clear dependence on the source-target distance, were found for fractures of all orientations.

Figure 10. **Magnitude 6 earthquake: Target fracture displacement as function of time**

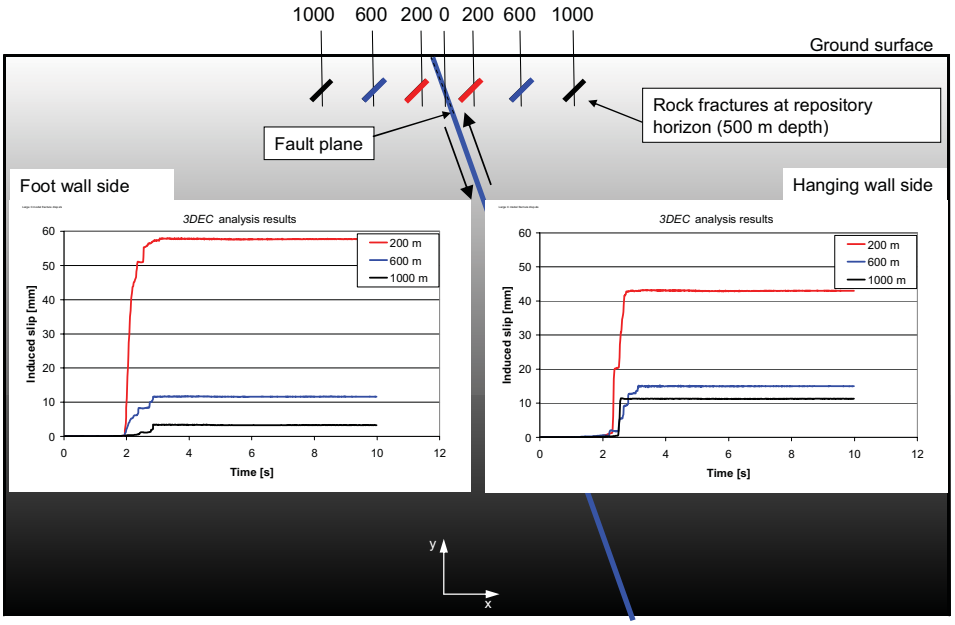

Figure 11 shows a summary of peak displacement results from all target fractures at distances 200 m and 600 m. The maximum peak displacement is about 80 mm. 95% of the fractures at the 200 m distance slip by less than 60 mm and 60% by less than 25 mm.

Figure 11. **Magnitude 6 earthquakes: Peak target fracture displacements**

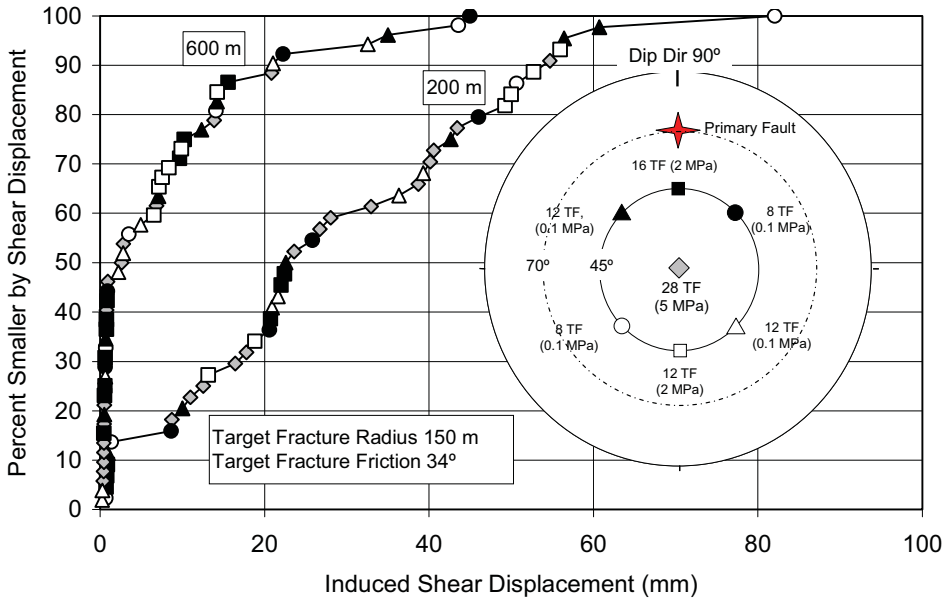

The inset in Figure 11 shows the orientation of the earthquake fault and the distribution of target fracture orientations, with a majority of horizontal fractures and with no vertical fractures. The stability margins of the target fractures are given in parentheses. It should be noted that the small

stability margins for fractures with dip directions 45º, 135º, 225º and 135º may turn out to be irrelevant because of the exaggerated stress anisotropy assumed at 500 m depth in the horizontal plane (cf. Figure 7).

The distribution of orientations is not related to site data. Note, however, that horizontal fractures are the most likely ones to intersect canister positions, whereas vertical fractures are the least likely ones. For both distances, 200 m and 600 m, it appears that fractures with small stability margins (circles and triangles) tend to displace more.

Magnitude 7.5 events

Figure 12 shows results from one of the magnitude 7.5 analyses. For the same target fracture orientation as in the corresponding figure (Figure 6) shown in the previous magnitude 6 section, the peak displacement is about 20 mm larger. Figure 13 shows a summary of results obtained from a couple of different magnitude 7.5 models, all with the same mechanical properties of rock and fractures and the same rupture propagation velocity, but with different *in situ* stress-depth relations and different schemes for ramping down the fault shear strength. Fast ramping (0.5 seconds, cf. Figure 8, left) appears to give large target fracture displacements, the fundamental parameter controlled being the fault slip velocity which is a quantity for which records from real earthquakes are available for comparison (cf. following section).

As of yet, there are no results from magnitude 7.5 models with target fractures dipping in other directions than 90º (same as fault) and 270º. Possibly, target fractures with the dip directions (and stability margins) tried in the magnitude 6 model (cf. Figure 11) would have slipped more.

Figure 12. **Magnitude 7.5 earthquake: Target fracture displacement as function of time**

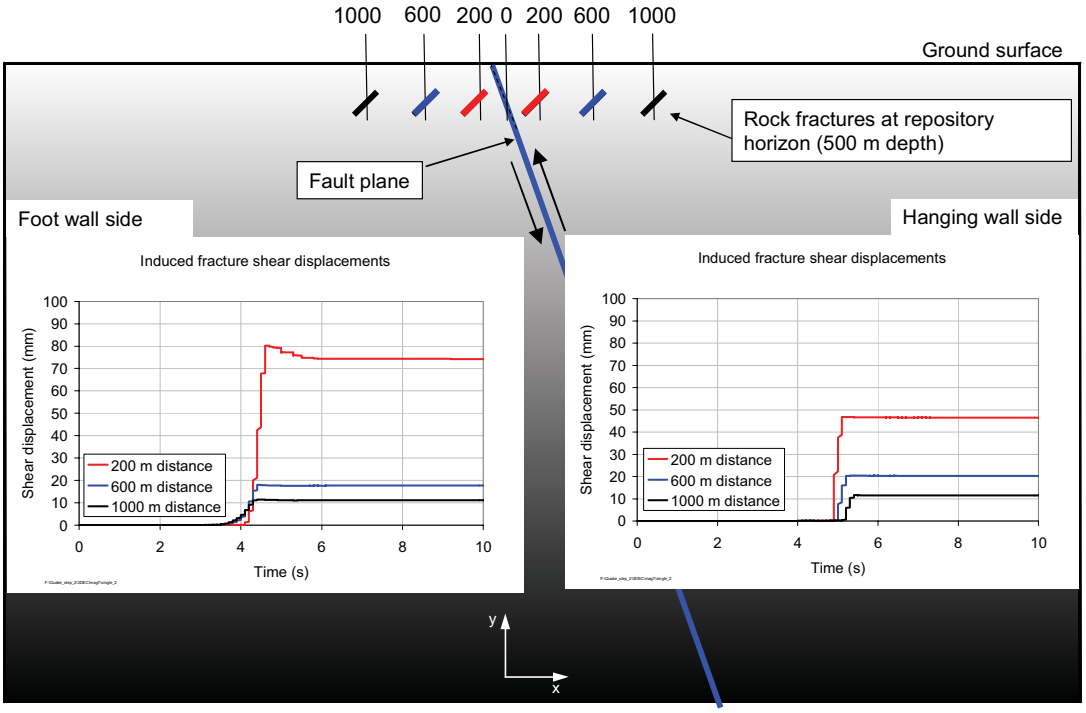

Figure 13. **Magnitude 7.5 earthquakes: Peak target fracture displacements**

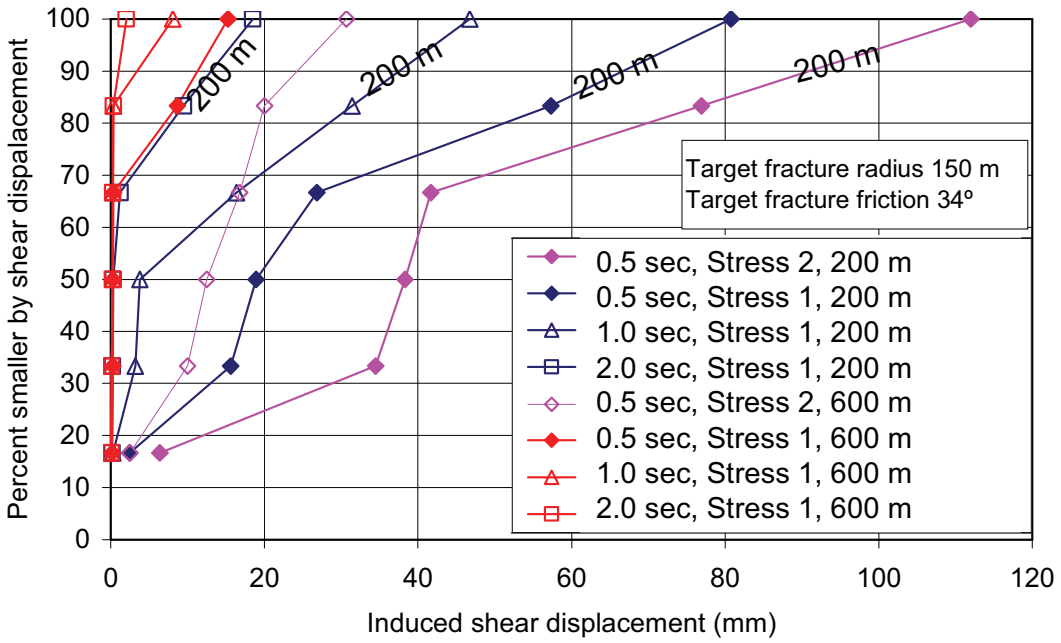

Conclusions and Discussion

The moment magnitude range considered here was 6.0 – 7.5. Out of the numerous 300 m diameter fractures with different orientations located at 200 m distance from the fault plane that were monitored, only one slipped more than 0.1 m in response to the fault slip (cf. Figure 13). For the magnitude 6 models no fractures slipped more than 82 mm. Obviously it will be important to establish if the largest displacements found in the different models are realistic, overestimates or underestimates.

Meshing and numerical precision

Numerical tests carried out with refined meshes have given insignificantly smaller induced displacements. However, with present-day computational capabilities it is not possible to do tests with significantly finer meshes to establish if there are systematic small overestimates in the results presented here. Analyses run in double precision give results that are effectively identical to the standard single precision results.

Relevance of the fault model

Figure 14 shows different 3DEC models plotted in a stress drop – slip velocity diagram. The stress drop is a much debated quantity, which is difficult to measure and for which estimates for one and the same event usually agree only within a factor of 4 or 5, depending on ambiguities in the underlying physics (Scholz, 2002). For the synthetic 3DEC earthquakes it is trivial to calculate the actual change in shear stress at every point of the fault (cf. Figure 8, left) and then integrate over the rupture area to find the average stress drop. This gives about 15 MPa for the magnitude 6 models and between 7 and 15 MPa for the truncated magnitude 7.5 models shown here. For real earthquakes one has to approximate the stress drop, for instance by the slip/width ratio as shown in the lower right inset of Figure (Scholz, 2002). Making the same approximation for all earthquakes modeled here and

comparing with corresponding stress drop approximations for the Lapland endglacial Lansjärv and Pärvie earthquakes suggests that our models are well on the conservative side. Slip/width ratios for the two endglacial earthquakes are based on estimates given by Muir Wood (1993) and Arvidsson (1996).

There are no maximum slip velocity records of any of the Lapland endglacial earthquakes. The 3DEC maximum slip velocities are instead compared with data reported for the 1999 Chi-Chi magnitude 7.6 earthquake by Ma *et al*. (2001) and Ma *et al*. (2003), and with the slip velocity of the 1992 magnitude 7.2 Landers, California, earthquake. Note that ground stations around the Chi-Chi earthquake recorded the largest values of ground velocity ever instrumentally measured (Ma *et al*., 2003). The Landers maximum slip velocity estimate is based on ground velocities reported by Wald and Heaton (1994).

Figure14. **Maximum fault slip velocity and average stress drop comparison**

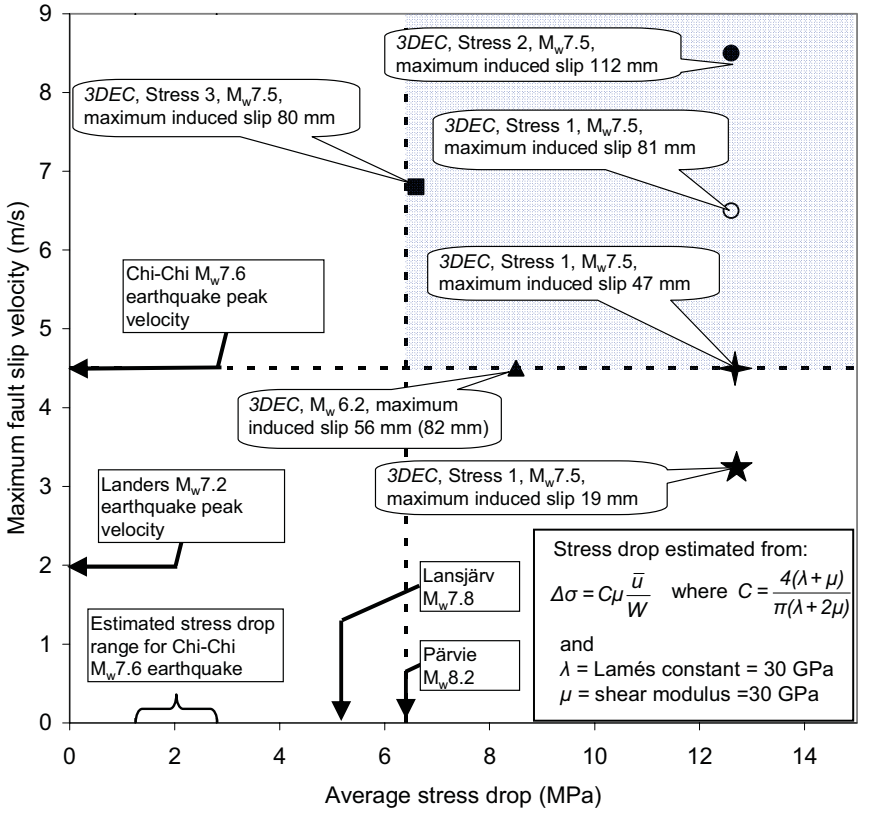

Stress drop is the most fundamental earthquake scaling parameter: measurements of slip, velocity, and acceleration can in principle be inverted for stress drop (Scholz, 2002). For the endglacial events we do, however, only have estimates of the average stress drop, not the maximum stress drop that would be associated with the highest potential of damage. For the Chi-Chi earthquake, for instance, Ma *et al.* (2001) estimated the stress drop to be 22 MPa if averaged over a 300 km^2 area around the high velocity region in the north part of the fault, whereas the fault average is not more than 1-3 MPa. Scholz (2006) confirms that local asperity stress drops may be one order of magnitude larger than the fault average stress drop, possibly 100 MPa and upwards. Therefore the maximum fault slip velocity may be a more reliable indicator of the potential for reactivation of nearby fractures than the average stress drop.

It appears that all 3DEC models giving target fracture displacement larger than 80 mm have not only average stress drops larger than the average stress drops estimated for the large Lapland endglacial earthquakes but also higher maximum slip velocities than those reported for the high-velocity Chi-Chi earthquake, i.e. all these models fall into the shaded area in the upper right part of the stress drop – velocity plot. Yet, with the exception of the magnitude 7.5 event plotted in the far upper right, the maximum target fracture displacement found in the models are below or well below the 0.1 m threshold. This suggests that, as far as the representation of the fault and rupture is concerned, the maximum 300 m diameter target fracture displacement for real earthquakes would probably be smaller than 80 mm at a distance of 200 m from the fault plane, irrespective of magnitude.

In situ stress and target fracture orientation

Depending on the stress state, the orientation and the fracture mechanical properties, target fractures can have larger or smaller stability margins, cf. Figure 7(right) and Figure 11. In the magnitude 6 models, target fracture displacements were systematically larger for fractures with dip directions other than 90º and 270º. The two values given for the magnitude 6 model in Figure 14 (i.e. 56 and 82 mm), regard the maximum displacement of fractures with 2 MPa and 0.1 MPa stability margins, respectively. As of yet, there has not been any systematic variations of the stability margin for differently oriented target fractures. The Mohr circle plots in Figure 15 show the effects of assuming the total minor horizontal stress to increase from the value assumed here, i.e. about 11.5 MPa (left) to about 25 MPa (right) at 500 m depth. Note that the minor horizontal stress is assumed to be parallel with the fault strike here and therefore unimportant to the fault behavior. Points on the semicircles and in the shaded areas correspond to possible fracture orientations. Obviously more fractures are in a failure state, or close to failure, for the stress models assumed in this study here (i.e. left) than there would be in the probably more realistic stress state shown to the right. From this point of view the initial stress state is conservative.

Figure 15. **Stability margins for different stress state variants**

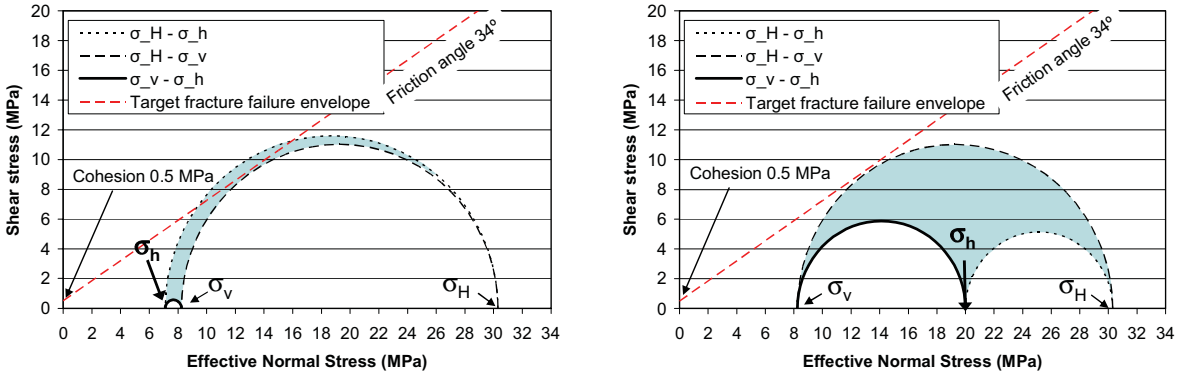

We do not know the actual stress levels of typical endglacial stress regimes. Here we have specified the residual fault shear strength to be zero and just calibrated the major horizontal stress to produce the average fault slip required to generate earthquakes of the intended moment magnitudes (cf. Eqs. 1 and 2). For real faults having non-zero residual strength, the initial major horizontal stress would have to be larger to produce the same average fault slip and the same seismic moment, i.e. the σH – σv Mohr circles (cf. Figure 15) would have to be larger, meaning that the dip range of fractures with small or zero stability margins would be larger.

Surrounding rock and target fractures

The intact rock between the explicitly modeled fractures (and between fractures and the fault plane) was assumed to be linear elastic, i.e. without any possibilities of energy dissipation. The consequences of this are difficult to estimate, but it is seems reasonable to believe that inelastic deformations, for instance within the fractured transition zone usually found around the core of large potential faults (Munier and Hökmark, 2004), would reduce the slip on target fractures outside that zone. There are also the effects of fracturing around the tips of slipping target fractures. During slip the stress concentrations around the tips of the slipping fracture will increase and eventually be sufficient to initiate fracture propagation, meaning that part of the strain energy will be expended on fracturing rather than on friction work. The process has been addressed qualitatively by La Pointe *et al.* (2000). As of yet there has not been any quantitative analyses showing the potential of this process to limit induced maximum displacements.

The target fractures were all assumed to be perfectly planar. This is obviously a conservative assumption. The strength properties were derived from data in the site models and should be regarded as reasonably realistic.

Final remarks

The considerations of the different aspects of the modeling approach and the modeling results listed above seem to support the supposition that the induced displacements calculated here are overestimates rather than underestimates. The work now in progress aims to establish or confirm this, most importantly by analyzing earthquakes that:

- are powered by more realistic stress fields, and
- have average stress drops not larger than those estimated for the Pärvie and Lansjärv events, and slip velocities not larger than the maximum velocity measured for the Chi-Chi earthquake.

Acknowledgement

The authors wish to acknowledge that this paper is based on work funded by the Swedish Nuclear Fuel and Waste Management Company (SKB)

References

Arvidsson, R, (1996), *Fennoscandian Earthquakes: Whole Crustal Rupturing Related to Postglacial Rebound*. Science 274, 744-746.

Bödvarsson R, B. Lund, R. Roberts and R. Slunga, (2006) *Earthquake activity in Sweden. Study in connection with a proposed nuclear waste repository in Forsmark or Oskarshamn*. SKB R-06-67. Svensk Kärnbränslehantering AB, Stockholm.

Börgesson L. and J. Hernelind, (2006) *Earthquake induced rock shear through a deposition hole. Influence of shear plane inclination and location as well as buffer properties on the damage caused to the canister*. SKB TR-06-43. Svensk Kärnbränslehantering AB, Stockholm.

Fälth B. and H. Hökmark, (2006), *Seismically induced slip on rock fractures*. SKB R-06-84. Svensk Kärnbränslehantering AB, Stockholm.

Fälth B. and H. Hökmark, (2007), *Seismically induced slip on rock fracture – expanded study with particular account of large earthquakes*, SKB R-07-xx. In prep. Svensk Kärnbränslehantering AB, Stockholm.

Hakami E. and S-O. Olofsson, (2002), *Numerical modelling of fracture displacements due to a thermal load from a KBS-3 repository*. SKB TR-02-08. Svensk Kärnbränslehantering AB, Stockholm.

Hökmark H., B. Fälth and T. Wallroth, (2006), T-*H-M couplings in rock. Overview of results of importance to the SR-Can safety assessment*. SKB R-06-88. Svensk Kärnbränslehantering AB, Stockholm.

Itasca, (2003), *3DEC – 3-Dimensional Distinct Element Code, ver. 3 User's Guide*. Itasca Consulting Group Inc, Minneapolis, USA.

La Pointe P.R, P. Wallman, A. Thomas and S. Follin, (1997), *A methodology to estimate earthquake effects on fractures intersecting canister holes*. SKB TR-97-07. Svensk Kärnbränslehantering AB, Stockholm.

La Pointe P.R, T. Cladouhos and S. Follin, (1999), *Calculation of displacements of fractures intersecting canisters induced by earthquakes: Aberg, Beberg and Ceberg examples*. SKB TR-99-03. Svensk Kärnbränslehantering AB, Stockholm.

La Pointe P.R, T. Cladouhos, N. Outters and S. Follin, (2000), *Evaluation of the conservativeness of the methodology for estimating earthquake-induced movements of fractures intersecting canisters*. SKB TR-00-08. Svensk Kärnbränslehantering AB, Stockholm.

Lagerbäck R., (1988), *Postglacial faulting and paleoseismicity in the Lansjärv area, northern Sweden*. SKB TR-88-25. Svensk Kärnbränslehantering AB, Stockholm.

Ma K-F. J. Mori, S-J. Lee and S.B. Yu, (2001), *Spatial and temporal distribution of slip for the 1999 Chi-Chi, Taiwan, earthquake*. Bulletin of the Seismological Society of America, Vol 91, No. 5, 1069-1087.

Ma K-F., E.E. Brodsky, J. Mori,C. Ji,T-R.A. Song and H. Kanamori, (2003), *Evidence for fault lubrication during the 1999 Chi-chi, Taiwan, earthquake* (Mw 7.6). Geophysical Research Letters 30(5): 4.

Muir Wood, R., (1993), *A review of the seismotectonics of Sweden*. SKB TR-93-13. Svensk Kärnbränslehantering AB, Stockholm.

Munier R. and H. Hökmark,(2004), *Respect distances. Rationale and means of computation*. SKB R-04-17. Svensk Kärnbränslehantering AB, Stockholm.

Munier R., (2006), *Using observations in deposition tunnels to avoid intersections with critical fractures in deposition holes*. SKB R-06-54. Svensk Kärnbränslehantering AB, Stockholm.

Scholz C., (2002), *The mechanics of earthquake and faulting*. 2nd Edition. Cambridge University Press, United Kingdom.

Scholz C., (2006), *Strength of faults and maximum stress drops in earthquakes*. In: report of the workshop on extreme ground motions at Yucca Mountain August 23-25, 2004. U.S. Geological Survey, Reston, Virginia.

SKB, (2005). *Preliminary site description*. Forsmark area – version 1.2. SKB R-05-18. Svensk Kärnbränslehantering AB, Stockholm.

SKB, (2006a), *Long-term safety for KBS-3 repositories at Forsmark and Laxemar – a first evaluation*. Main Report of the SR-Can project. SKB TR-06-09, Svensk Kärnbränslehantering AB, Stockholm.

SKB, (2006b), *Preliminary site description. Laxemar subarea – version 1.2*. SKB R-06-10. Svensk Kärnbränslehantering AB, Stockholm.

Slunga R., (1991), *The Baltic Shield earthquakes*. Tectonophysics, Vol. 98, 323-331.

Wald D.J. and T.H. Heaton, (1994), *Spatial and temporal distribution of slip for the 1992 Landers, California earthquake*. Bulletin of the Seismological Society of America, Vol 84, No. 3, 661-691.

Wells D.E. and K.J.Coppersmith, (1994), *New empirical relationships among magnitude, rupture length, rupture width, rupture area, and surface displacement.* Bulletin of the Seismological Society of America, 84(4), 974.1002.

BUFFERING AGAINST INTRUSION OF GROUNDWATER OF UNDESIRABLE COMPOSITION

P. Pitkänen, A. Luukkonen, S. Partamies
VTT, Finland

Abstract

Favourable hydrogeochemical conditions in a geological repository for spent nuclear fuel might be unbalanced by intrusion of undesirable water compositions. Such conditions have been triggered by hydrogeological transients caused by glacial cycles in Fennoscandian Shield. Deglaciation and marine stages are such changes, which could have introduced either dilute, low pH and oxic melt water or marine source water for SO_4 reduction producing dissolved sulphide, and have unbalanced favourable hydrogeochemical conditions in the geological past. It appears that groundwater system has a sufficient buffering capacity against these natural perturbations, and is able to stabilise chemical conditions. Current understanding of hydrogeochemical system does not support notable dilution and indicates strong buffering capacity against O_2 infiltration or low pH water. However, the information cannot unambiguously prove that oxygen has not reached deep bedrock and one major uncertainty is associated with existence and rate of marine sulphate reduction. Therefore focussed fracture mineral studies and field investigations with modelling excercises are desirable to verify the stability of favourable hydrogeochemical conditions.

Introduction

Stability of hydrogeochemical conditions are of importance for the durability of the engineered barriers (canister, bentonite buffer and other sealing materials) and for the solubility and migration of radionuclides. In groundwater the most critical chemical parameters for safety are salinity, pH, and redox conditions. Highly saline waters (TDS > 50 g/L) can be harmful by promoting the corrosion of metals, the solubility of radionuclides and by decreasing the swelling properties of clay minerals in bentonite. Extremely dilute water with very low cation contents (< 1 mmol/L) may cause dispersion of bentonite in the form of colloids. Exceptionally low (<5) or high pH (>10) conditions tend to increase radionuclide solubilities and may activate weathering and alteration processes of clay minerals in bentonite. Uncommon redox conditions in deep crystalline bedrock, such as the presence of dissolved oxygen or high sulphide concentrations, are also detrimental for the corrosion of metals and enhance the solubility of some actinides.

Hydrogeochemical conditions in crystalline rock observed, for instance in Finnish, Swedish and Canadian study sites are generally favourable in depths considered suitable (400 - 700 m) for safe disposal of spent nuclear fuel (Nordstrom *et al.*, 1989; Vieno & Nordman, 1999; Puigdomenech, 2001; Gascoyne, 2004; Frape *et al.*, 2005; Laaksoharju *et al.*, 2008). The present-day hydrogeochemical conditions at potential repository depths at Olkiluoto, the site for deep geological disposal of spent nuclear fuel in Finland also provide the conditions for long-term repository safety (Pitkänen *et al.*, 1999, 2004, Andersson *et al.*, 2007). Slightly alkaline pH, reducing conditions with low dissolved

sulphide, and tolerable salinity at about 400 to 500 m depth are generally favourable for long canister lifetimes, bentonite buffer stability and reduced radionuclide solubilities. However, the chemical conditions in groundwater may change. Dilute, oxic, low pH groundwaters from above, highly saline groundwater deep in the bedrock (below 800 m depth) or groundwater with high sulphide levels may be formed and transported to the repository level. Therefore, it is important to discover whether the hydrogeological/geochemical system has adequate buffering capacity to stabilise favourable conditions.

In general, chemical groundwater conditions are stable at depth at Olkiluoto and reactions and transport processes proceed very slowly (Pitkänen *et al.*, 2004). However, chemical interactions may enhance and thus may also consume the buffering capacity and destabilise hydrogeochemical system, if groundwaters with different chemical states are intruded and mixed in the bedrock. The transient may be driven by external natural processes and lead to a mixing of different water types from different parts of the geosphere. Climate change may have a marked effect on the prevailing stable groundwater conditions over the long-term, increasing groundwater flow and, therefore, the potential for mixing. Glacial cycles, deglaciation and conjoined marine stages with land uplift are such changes which could have introduced undesirable water compositions (low saline and pH, oxic melt water, marine source water for SO_4 reduction) and have unbalanced hydrogeochemical stability in the geological past. It is necessary, therefore, to have a good understanding of the hydrogeochemical evolution of the site, regarding former buffering induced by the mixing of groundwaters.

Destabilising palaeohydrogeological events

Crystalline bedrock at Fennoscandian Shield has undergone polyphase hydrothermal events during the Precambrian and early Phanerozoic. The imprints of these events can be recognized from the evidence of complex alteration in the walls of fractures, and such events may also have influenced the current groundwater chemistry, particularly the high salinities observed in great depths, which correspond with highly saline fluid inclusions observed occasionally in fracture calcites (Blyth *et al.*, 2000, Gehör *et al.*, 2002, Frape *et al.*, 2005). Also, understanding the transient glacial/postglacial evolution in the Baltic Sea region during the Holocene is vital when evaluating hydrogeochemical data in deep drillholes, since it provides constraints on the possible groundwater types that may occur in the bedrock (Figure 1).

The interpretation of the glacial/postglacial events that have affected the groundwater composition around the Baltic Sea in the Fennoscandian Shield is based on Quaternary geological information from various sources, including Eronen *et al.* (1995), Donner *et al.* (1999).

Complete Weichselian deglaciation started about 11 500 years ago (Figure 1), and ice sheet retreated quickly from Salpausselkä marginal deposit formed during the preceding millennium. Significant parts of southern Finland were below fresh palaeo-Baltic sea after the deglaciation. Glacial meltwater close to the retreating ice margin was able to infiltrate the bedrock under considerable pressure.

The Olkiluoto site also remained submerged during the early stages of the fresh water and the saline Littorina Sea (starting around 8 500–8 000 years ago). During the main part of the Littorina stage, between about 8 000 and 4 500 years ago, when the sea at Olkiluoto had a depth of about 50 to 30 m, total dissolved solids (TDS) in the seawater was about 4‰ higher than in the modern Baltic Sea at the Finnish coast (Donner *et al.*, 1999). The denser, brackish seawater of the Littorina Sea could have percolated into the bedrock by gravity, resulting in a density turnover, because the density of the groundwater in the bedrock had probably decreased due to meltwater infiltration, at least in its upper part.

Figure 1. **Postglacial shoreline in southern Finland from about 11 500 years ago (BP) until the present (after Eronen *et al.*, 1995). Almost whole Finland was covered by the Weichselian ice sheet 11 500 years ago, when ice margin located at Salpausselkä marginal deposit. Marine regression and uplift resulted mainly from crustal rebound after glaciation. Also shown are sites in Finland whose hydrogeochemical conditions are found to be related to their situation relative to deglaciation and Baltic Sea evolution**

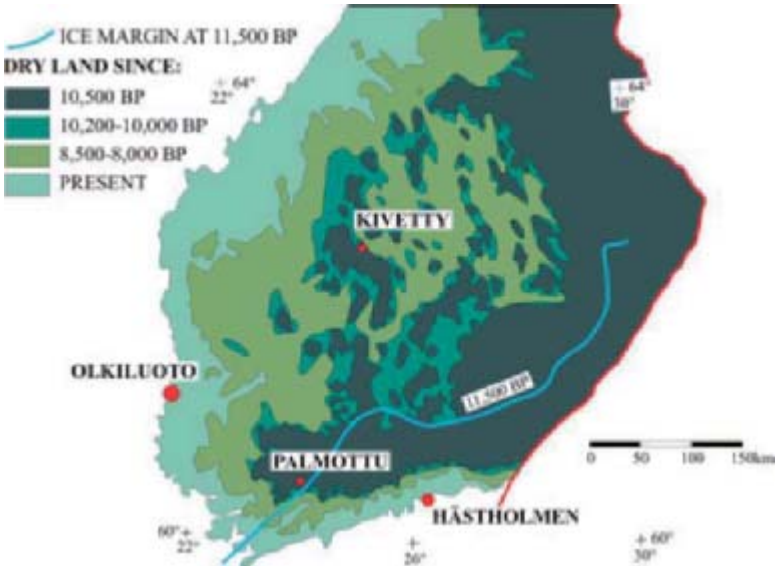

As a result of continuous land uplift, Olkiluoto Island begun to emerge from the Baltic Sea about 3 000–2 500 years ago and currently the post-glacial uplift at the site is about 4-6 mm/yr (Eronen *et al*., 1995). The infiltration of fresh meteoric water (precipitation) successively formed a lens on top of the saline water because of the lower density of fresh water. Infiltrating meteoric water is aggressive, containing carbonic acid and oxygen, due to aerobic respiration in the unsaturated organic soil layer. Thus, infiltration may also induce weathering processes in the bedrock.

Hydrogeochemical indications of hydrogeological perturbations

The groundwater chemistry over the depth range 0-1 000 m at Olkiluoto is characterised by a significant range in salinity. Fresh groundwater with low TDS (≤ 1 g/l; Davis 1964) is found only at shallow depths, in the uppermost tens of metres (Figure 2a). Brackish groundwater, with TDS up to 10 g/l dominates at depths, varying from 30 m to 450 m. Fresh and brackish groundwaters are classified into three groups on the basis of characteristic anions (Figure 2), which also reflect the origin of salinity in each groundwater type. Chloride (Figure 2b) is normally the dominant anion in all bedrock groundwaters, but the near-surface groundwaters are also rich in dissolved carbonate (high DIC in Fresh/Brackish HCO_3 type, Figure 2c), the intermediate layer (100-300 m) is characterised by high SO4 concentrations (Brackish SO_4 type, Figure 2d) and the deepest layer solely by Cl (Brackish Cl type), where SO_4 is almost absent. In crystalline rocks high DIC contents are typical of meteoric groundwaters which have infiltrated through organic soil layers, whereas high SO4 contents indicate a marine origin in crystalline rocks without SO_4 mineral phases. Fairly low δ13C values of DIC (-25 to -15‰ PDB) and high partial pressures of CO_2 (frequently Log PCO_2 > -2) also indicate mainly soil derived carbonate in HCO_3 type groundwaters (Clark & Fritz 1997). Saline groundwater (TDS > 10 g/l) dominates below 400 m depth. The highest salinity observed so far is 84 g/L. Sodium and calcium are the dominant cations in all groundwaters and Mg is notably enriched in SO_4-rich groundwaters, supporting their marine origin.

The position of stable isotope compositions of groundwaters relative to the global meteoric waterline (GMWL) indicates potential chemical and physical conditions and processes (e.g. Clark & Fritz, 1997; Frape *et al.,* 2005), which are indicated in Figure 3.

The stable isotopic composition of groundwater is in most cases controlled by meteorological processes and the shift along the GMWL reflects climatic changes in precipitation. Cold climate precipitation has a lighter isotopic composition (more negative values), whereas warmer climate shows a heavier composition. A shift to the right or below the GMWL typically indicates evaporation in surficial waters, which are enriched due to fractionation in heavier isotopes, particularly 18O, relative to the vapour phase. Therefore, seawater composition is, for example, below the GMWL. The shift above the GMWL is unusual and observed mainly in shield brines. In order to produce such strong fractionation in oxygen and hydrogen isotopes, it has been proposed that this is due to effective primary silicate hydration under a low water-rock ratio (Clark & Fritz 1997; Gascoyne, 2004; Frape *et al.*, 2005).

Another combination of conservative parameters reflecting the origin are Br and Cl ratio of groundwaters (Figure 4). The ratio is almost constant in marine waters (current oceanic value 0.0034). Relative enrichment of Br in brackish Cl and saline groundwaters might be dated back to ancient fractionation between Br and Cl, either in hydrothermal fluid or in evaporation basin before infiltration, under which conditions Cl is preferentially transferred in solid phases and Br remains in the fluid phase (Nordstrom *et al.,* 1989, Frape *et al*., 2005).

Figure 2. **TDS, Cl, DIC and SO_4 concentrations as a function of depth of Olkiluoto**

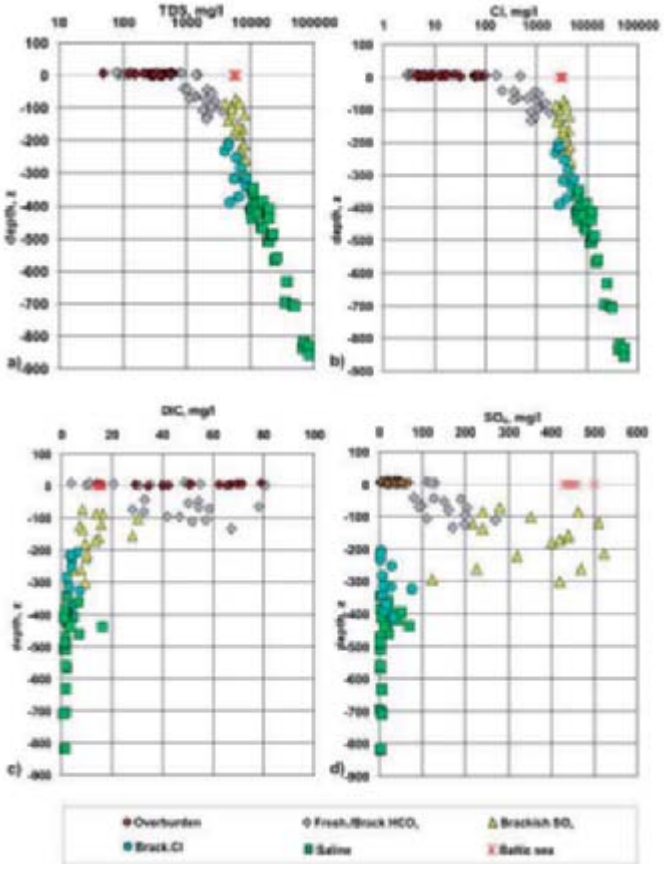

Figure 3. **Relationship between $\delta^{18}O$ and $\delta^{2}H$ in Olkiluoto water samples. Arrows depict the compositional changes caused by the named conditions. Global meteoric water line (GMWL) after Craig (1961)**

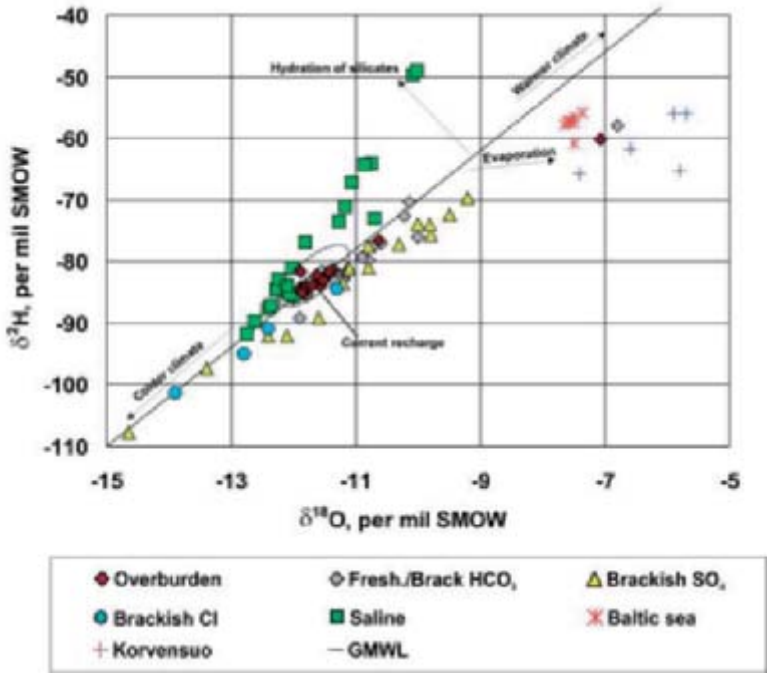

Figure 4. **Relationship between Br-Cl ratio and depth in Olkiluoto groundwater samples**

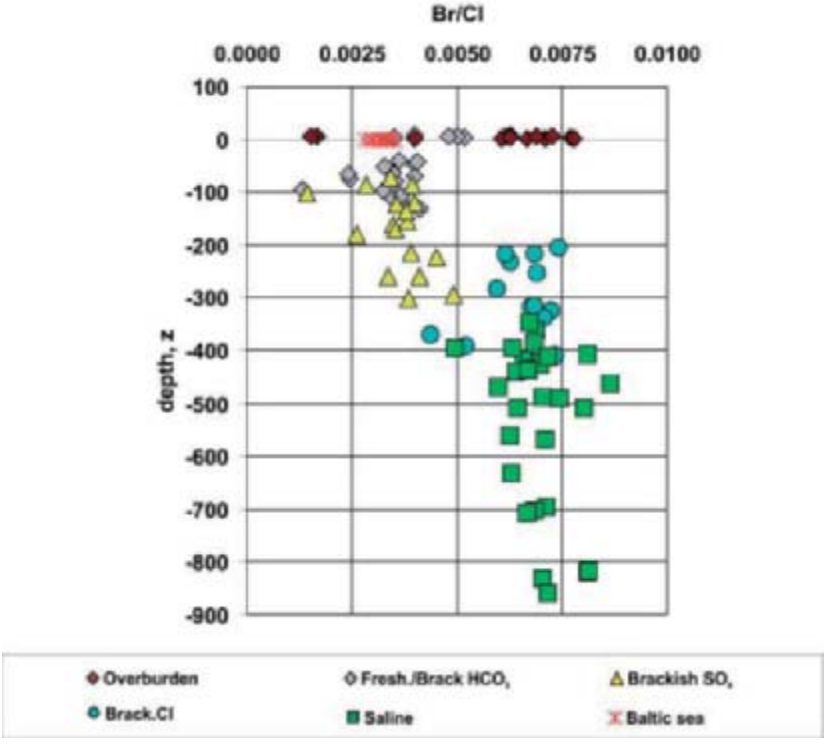

The interpretations of chemical and isotopic data (Pitkänen *et al*., 2004, Andersson *et al.,* 2007 and Figures 2 to 4) indicate, however, that there are water types from at least six different sources influencing current groundwater compositions at the site. They originate from different periods, ranging from modern times, through former Baltic stages, to pre-glacial times:

modern	• Meteoric water, which infiltrated during terrestrial recharge (during the last 0 – 2 500 a), plots over a limited area along the GMWL in Figure 3. Shallow groundwaters from overburden and bedrock (Fresh HCO_3-type) are the best representatives of this source, but clear imprints of meteoric water mixed with former groundwaters can be seen down to 100 m to 150 m depth (Brackish HCO_3-type). These water types normally contain tritium and radiocarbon varies from 100 pmC to 50 pmC resulting from isotopic dilution.
	• Seawater from the Gulf of Bothnia (0 – 2 500 a ago) has a signature showing evaporative effects. The influence of current seawater can be seen as a slight increase in salinity in fresh HCO_3-type samples.
	• Water in the Korvensuo reservoir at Olkiluoto (domestic water used in drilling – originally river water) shows an even stronger evaporative tendency than seawater in Figure 3. The signature of the reservoir is observed from a few shallow, fresh groundwater samples in the vicinity of the reservoir.
relic	• The influence of Littorina seawater (infiltrated 2 500 – 8 500 a ago) dominates in brackish SO_4-type groundwater, as well being observable in brackish HCO_3-type samples. Both groundwaters tend to shift to the right from the GMWL towards the current seawater composition (Figure 3). The marine origin of dissolved solids is indicated by the marine signatures of Br/Cl (Figure 4), SO_4/Cl and Mg/Cl ratios, and the Littorina origin by a higher salinity than in modern Baltic water and a clearly lower radiocarbon content than in HCO_3-rich groundwaters. Suplhur-34 of SO_4 is generally slightly higher than in marine SO_4 value, i.e. +20‰ CDT, which indicates minor microbial reduction of originally marine derived SO_4 in groundwaters.
	• The colder climate meteoric water signature in the groundwater data (Figure 3) probably results from the inclusion of glacial meltwater (more than 10 000 years ago). The influence is observable both in brackish SO_4-type groundwater and in brackish Cl-type groundwaters. The latter type shows similar non-marine chemical signatures to saline groundwater (e.g. Br/Cl ratio is twice the marine signature in the brackish SO_4-type, Figure 4) and a further depleted radiocarbon content, which indicates a longer residence time than brackish SO_4-type groundwater.
	• The stable isotopic signature in saline groundwater (Figure 3) above the GMWL indicates strong hydration of silicates. There are several indications for assuming an extremely long residence time for saline water. In particular, the observations from fracture infillings and fluid inclusion studies indicate elevated temperatures for hydration and a saline source water. Therefore, the saline water source (probably brine) intruded and/or formed under the influence of hydrothermal fluids, which, according to present geological knowledge, prevailed possibly during the early Phanerozoic under thick sedimentary cover (Kohonen & Rämö, 2005) or during the Precambrian. The original brine end-member has later been diluted with meteoric water from precipitation in a colder climate than at present. Brackish Cl-type groundwaters represent the end-product of this dilution.

It has been discovered that the glacial/postglacial geological information is reflected in the deep groundwater chemical and isotopic compositions, not only at Olkiluoto but at several other sites in Finland (Figure 1) and Sweden (Pitkänen *et al.*, 1998, 2001, 2004; Laaksoharju and Wallin, 1997; Smellie *et. al.*, 2002; Laaksoharju *et al.,* 2008). Similar Littorina seawater infiltration as in Olkiluoto has been observed in several coastal locations in Finland and Sweden.

Correspondingly glacial melt water intrusion has frequently interpreted from different sites. The exact penetration depth is still unknown, but at present the glacial maximum varies in the depths of 100 to 500 m according to 18O isotopic data of groundwaters in sites in Figure 1 (Pitkänen *et al.,* 1998, 2001, 2004; Smellie *et al.,* 2002). The maximum is between 100 and 200 m depth at Olkiluoto. The fraction of melt water seems to vary being highest in places near the Salpausselkä and minor in supra-aquatic areas. Infiltrating fresh meltwater, potentially contains oxygen, though no signals of such oxidation have been observed so far for instance at Olkiluoto and deep groundwaters are anaerobic, in general.

Buffering against infiltration

Signatures of unfavourable hydrogeological perturbations caused by glacial cycle are fairly common in hydrogeochemical systems in Fennoscandian Shield. As a scenario, abrupt dilute, oxidative and low pH waters penetration with glacial melt might intrude to repository depths. Another marine derived scenario indicates that high sulphide concentrations could develop underground by microbial reduction of sulphate.

Hydrodynamic conditions have evidently controlled intrusion depths of infiltrating water types and mixing of dilute waters (glacial melt or precipitation) in existed groundwaters has been sufficient alone to increase salinity on acceptable level at Olkiluoto. Comparison of δ18O and Cl data (Figure 5) indicates that waters infiltrated during deglaciation or postglacial time have not mixed significantly in deep saline groundwater system. The linear dilution of saline groundwater could be solved by two end-member mixing with brine reference and fresh to brackish water with δ18O between -12 and -13‰. This fresh to brackish water could be a constant mixture of other fresh and brackish reference waters (or their original end-members). However, a high Br-Cl-ratio, extremely low HCO_3 and SO_4-contents and a mixing trend in stable isotopic composition of saline and brackish Cl-type groundwaters (Figures 2-4), indicate that these groundwater types do not contain any significant fraction of postglacial water components, i.e. Littorina-derived seawater and meteoric recharge. Therefore, it can be assumed that saline groundwater has also not been diluted by pure glacial meltwater. The dilution of saline groundwater is, accordingly, due to an older event than the last deglaciation and may be the sum of several fresh water infiltrations, glacial meltwater, as well as meteoric recharge, for example during earlier Quaternary glacial cycles.

As the Cl content decreases still further in brackish Cl type groundwaters, δ18O values clearly drop relative to the saline groundwater dilution trend (Figure 5). These samples plot along the mixing trend between an estimated Littorina seawater composition (Pitkänen *et al.*, 2004) and a potential glacial meltwater composition, down on the vertical axis (practically no Cl in meltwater). The association with Littorina mixing and the contrast with brine dilution also indicates that the meltwater was derived from the Weichselian glacier and that its main influence was limited to the upper 300 m.

The infiltration of Littorina seawater clearly increases both salinity and δ18O-values in brackish SO_4-type groundwaters (Figure 5). The highest values are measured in groundwaters sampled from depths between 100 to 300 m, the same range from which less saline brackish Cl-type and HCO_3-type groundwaters are observed (Figure 2). This is probably caused by the heterogeneous transmissivity of

hydrogeologically active zones - the former groundwater type may represent less transmissive pockets and the latter highly transmissive zones in the bedrock.

The major hydrogeological zones in the bedrock of Olkiluoto are subhorizontal, which have probably been able to limit deep infiltration from surface. Another coastal site with saline groundwater, Hästholmen (Figure 1) is characterised also by vertical zones, where clear glacial melt signatures reach to 400 m depth. It seems that hydrogeological system has sufficient stability against environmental changes, because Fennoscandian area has encountered several glacial cycles during Quaternary without significant dilution or any marine signatures of deep saline groundwater system at Olkiluoto.

Figure 5. **$\delta^{18}O$ versus Cl concentrations in Olkiluoto groundwaters. Groundwater samples referring to potential end-members are denoted [Littorina estimated by Pitkänen *et al.* (2004)]**

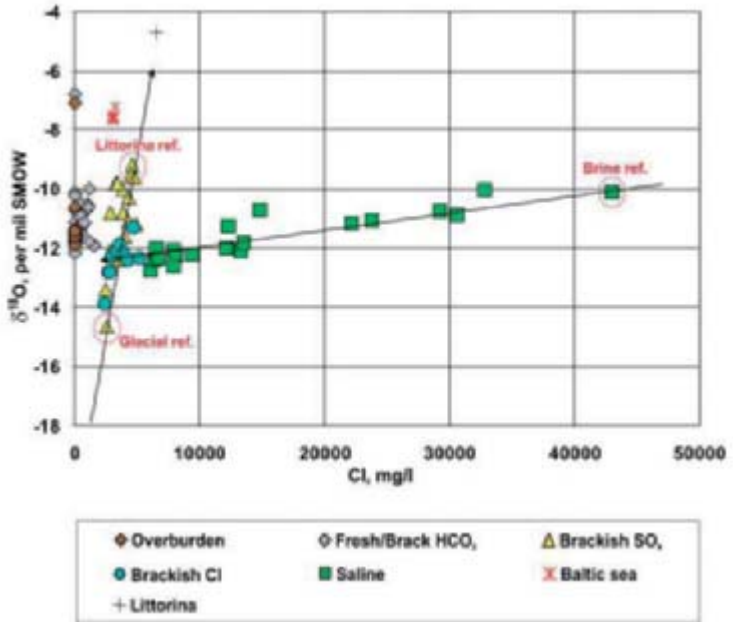

Weathering processes induced by dissolved gases, i.e. CO_2 and O_2, dominate typically in shallow, low pH groundwater recharging through the organic soil layer into the inorganic overburden and bedrock. Oxygen is derived from the atmosphere, whereas CO_2 is mainly generated by aerobic oxidation of organic carbon, which probably consumes the majority of the oxygen from recharging water in current conditions. The rest of the infiltrating oxygen is probably used in oxidizing mineral sulphides and ferrous iron in silicates in near-surface weathering. Oxygen intrusion with glacial melt may have more potential to create a redox perturbation deep in the bedrock than the present infiltration (Puigdomenech, 2001). Hydrogeochemical system has significant buffering capacity against O_2 infiltration. In addition the organic compounds in overburden, pyrite is a frequent fracture mineral in all depths (ca. 0.6 mols/m2 of pyrite within open fracture surfaces) and high CH_4 content is typical in deep groundwater below SO_4-rich groundwaters. Iron sulphides react easily with oxygen producing iron oxyhydroxides as reaction product. However, no signs of such oxidations have been observed deep in the bedrock at Olkiluoto and actually they are limited to the uppermost few meters near the surface (Gehör, 2007). Recently corroded pyrites in fractures are lacking as well. Methanotrophs can oxidise CH_4 and consume dissolved O_2 producing CO_2. The oxidation of CH_4 should have a strong decreasing effect on the δ13C signature of dissolved carbonate or precipitating fracture calcites, if oxidation is a significant process, because δ13C in CH_4 is generally less than -40‰ PDB down to

700m depth at Olkiluoto (Pitkänen & Partamies, 2007). However, methane derived very low δ13C values are rare in DIC and none observed in the late stage fracture calcites, which show particularly high even positive δ13C values (Blyth *et al.,* 2000, Gehör *et al.,* 2002). Those few observations in groundwater have been indicated to result from microbial anaerobic oxidation of CH_4 with reduction of SO_4. Fracture mineral studies have been systematic, but intensive studies focussed on the outermost, latest fracture in fills with detailed microscopic and isotopic analyses have been tentative so far. Such studies are, however, planned to concentrate on potentially major infiltration zones.

Hydrogeochemical and C-isotopic interpretations, solubility calculations, as well as fracture mineral studies, indicate that pH seems to be dominantly controlled by the thermodynamic equilibrium with calcite in fractures. Calcite is the most common fracture-filling mineral occurring generally in fractures from shallow depths (Gehör, 2007) and there are indications that it may also occur in the overburden layer (Pitkänen *et al.,* 2004). Calcite is dissolving in the recharge zone due to high contents of dissolved CO2 in groundwater, quickly approaching equilibrium at shallow depths, as pH neutralises (Figure 6). Carbon-13 in DIC increases rapidly in HCO_3-rich groundwaters (tritium containing) from organic derived values (about -25‰ PDB) along with decreasing radiocarbon from about 100 pmC to about 50 pmC level supporting calcites dominant role in buffering pH and alkalinity against acid recharge.

Figure 6. **The variation of pH and calculated calcite saturation indices with depth in Olkiluoto groundwaters**

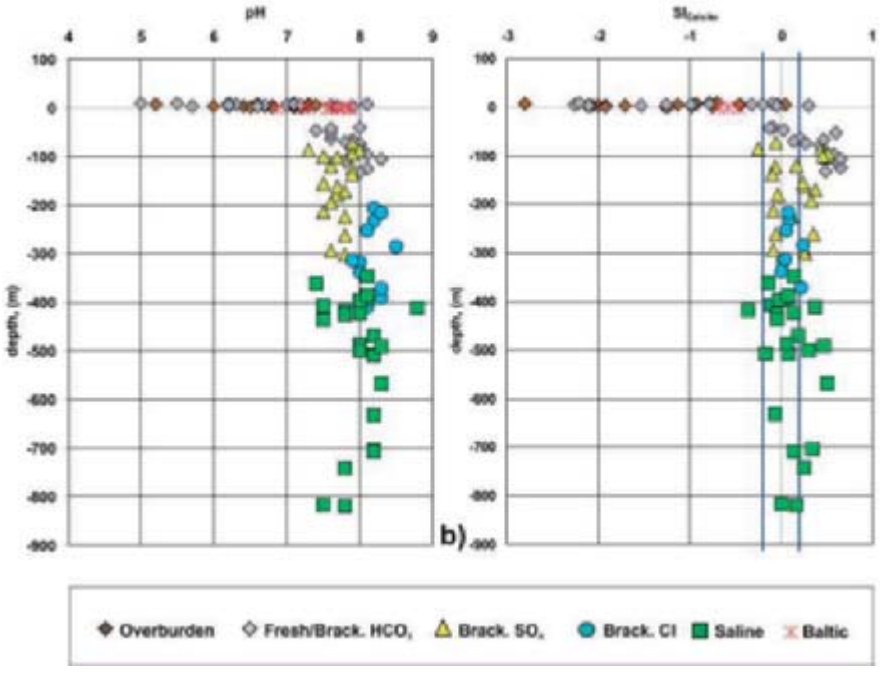

The baseline hydrogeochemical system at Olkiluoto seems to include another thermodynamically metastable interfaces in addition to aerobic-anaerobic interface in infiltration zone (Pitkänen *et al.,* 2004, Pitkänen & Partamies, 2007). At this lower interface SO_4-rich, marine-derived groundwater (Littorina) is mixed with methane to result, in places, in exceptionally high levels of dissolved sulphide (Figure 7), as microbially-mediated reaction product, which may precipitate as pyrite. Reactive iron buffer precipitating sulphide is weak, because iron oxyhydroxides are lacking due to strongly reducing nature of bedrock at Olkiluoto. Kinetics of silicate iron fraction is only poorly reactive towards dissolved sulphide (Raiswell and Canfield, 1996).

Figure 7. **Dissolved sulphate, methane and sulphide contents with depth at Olkiluoto**

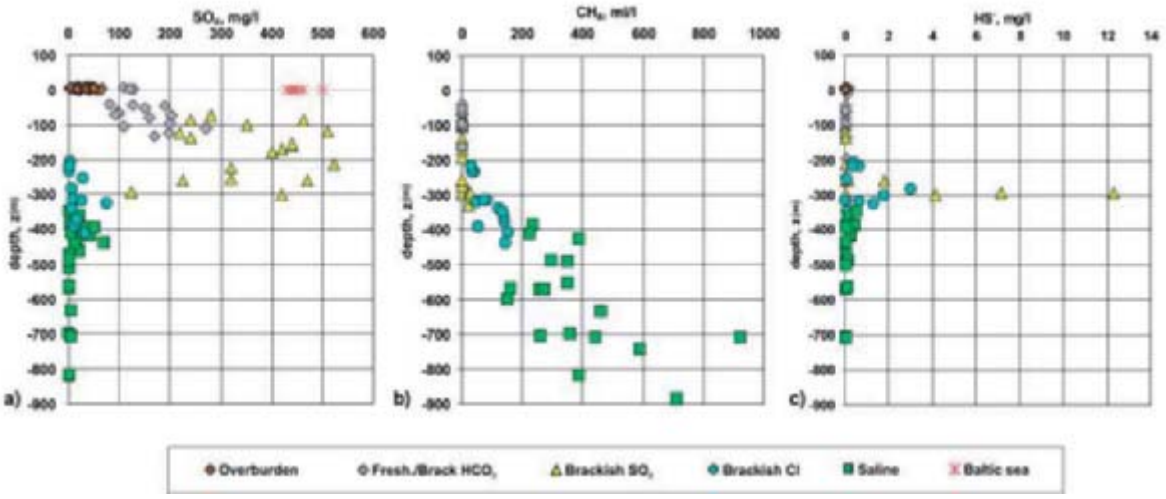

One major uncertainty which needs further investigation is associated with the existence and rate of sulphate reduction. The process is evident and intensive in the interface between SO_4- and CH_4-rich groundwaters, producing dissolved sulphide. However, the reduction process and the increase of dissolved sulphide seems to be retarded, but the actual reason for this is unknown. The reason could be hydrogeological (limited mixing of water types or limited upward diffusion of CH_4) or microbiological (due to complex and/or slow mechanism which uses CH_4 as a reducer or lack of nutrients). Sulphide precipitation may be one explanation. However, source of iron remains enigmatic (lack of oxyhydroxides). Marine signatures are lacking from deep saline groundwater similarly as glacial melt signatures, therefore system could be hydrodynamically buffered. As a summary, the complete causality at the interface is unclear and should be worked out in order to evaluate the potential safety risks.

Conclusions

It appears that groundwater system at Olkiluoto has a sufficient buffering capacity against natural perturbations of undesirable water compositions, and is able to stabilise chemical conditions that could be harmful for long term repository safety. Current understanding of hydrogeochemical system does not support notable dilution and indicates strong buffering capacity against O_2 infiltration with glacial melt deep in the bedrock. Similarly pH buffer, principally formed by fracture calcites seems to be sufficient. However, the information cannot unambiguously prove that oxygen has not reached deep bedrock or repository depths: Iron oxyhydroxides, the potential imprints of aerobic conditions may have been consumed later in microbial SO_4 reduction process by pyrite precipitation. Carbonate isotopic data from fracture calcites, detailed mineralogical and isotopic data from fracture pyrites might not yet be on reliable level. Therefore focussed fracture mineral studies are desirable to verify stability of hydrogeochemical system (Andersson *et al.*, 2007). Important information may also be gained by field studies in the vicinity of continental ice edge linked with hydrogeological modelling exercises. Appropriate context could be either marginal deposits representing past stagnant continental ice margin or existing one (e.g. Greenland), however, hydrogeological and geochemical correspondence to perform as an analogue should be clarified.

The issue of microbial reduction of marine intrusion derived SO_4 is considered important (Andersson *et al.*, 2007) and requires both field investigations and the development of hydrogeochemical modelling tools coupling biogeochemical processes in reactive transport code.

Isotopic studies of fracture minerals may also give further information on microbial SO_4-CH_4 redox activity due to past marine stages during Quaternary.

References

Andersson J., H. Ahokas, J.A. Hudson, L. Koskinen, A. Luukkonen, J. Löfman, V. Keto, P. Pitkänen, J. Mattila, A.T.K. Ikonen and M. Ylä-Mella, (2007). *Olkiluoto Site Description 2006*. Posiva Oy, Eurajoki, Finland. POSIVA 2007-03, 546 p.

Blyth, A., S. Frape, R. Blomqvist and P. Nissinen, (2000), *Assessing the past thermal and chemical history of fluids in chrystalline rock by combining fluid inclusion and isotopic fracture calcites.* Applied Geochemistry 15, p 1417-1437.

Clark, I. and P. Fritz, (1997), *Environmental isotopes in hydrogeology*. Lewis Publishers, Boca Raton, 328 p.

Craig, H., (1961), *Isotopic variations in meteoric waters*. Science 133, p. 1702.

Davis, S.N., (1964), *The chemistry of saline waters*. In: Krieger, R.A. – Discussion. Groundwater, vol 2(1), 51.

Donner, J., T. Kankainen and J.A. Karhu, (1999), *Radiocarbon ages and stable isotope composition of Holocene shells in Finland*. Quaternaria A:7, 31-38.

Eronen, M., Glückert, G., van de Plassche, O., van de Plicht, J. & Rantala, P. 1995. Land uplift in the Olkiluoto-Pyhäjärvi area, southwestern Finland, during last 8000 years. Waste Commission of Finnish Power Companies, Helsinki, Finland. Report YJT -95-17, 26 p.

Frape, S.K., A. Blyth, R. Blomqvist, R.H. McNutt and M. Gascoyne, (2004), *Deep fluids in the continents: II*. Crystalline rocks. Treatise on Geochemistry, 5, 541–80.

Gascoyne, M., (2004), *Hydrogeochemistry, groundwater ages and sources of salts in a granitic batholith on the Canadian Shield, southeastern Manitoba*. Applied Geochemistry 19, 519-560.

Gehör, S., (2007), *Synthesis of the fracture mineral study of the Olkiluoto site. Posiva Oy, Eurajoki, Finland*. Working Report (in press).

Gehör, S., Karhu, J., Kärki, A., Löfman, J., Pitkänen, P., Ruotsalainen, P. & Taikina-aho, O. 2002. Fracture calcites at Olkiluoto: Evidence from Quarternary Infills for Palaeohydrogeology. Posiva Oy, Eurajoki, Finland. POSIVA 2002-03, 118 p.

Kohonen, J. and O.T. Rämö, (2005), *Sedimentary rocks, diabases, and late cratonic evolution*. Developments in Precambrian Geology 14, 565 – 603.

Laaksoharju, M., J. Smellie, E-L. Tullborg, M. Gimeno, J. Molinero, I. Gurban and L. Hallbeck, (2008), *Hydrogeochemical evaluation and modelling performed within the site investigation programme*. Applied Geochemistry (to be published).

Laaksoharju, M. and B. Wallin, (1997), *Integration of hydrochemical and hydrogeological models of Äspö. Proceedings of the second Äspö International Geochemistry Workshop*, June 6-7, 1995. SKB, International Co-operational Report 97-04.

Nordstrom, D.K., J.W. Ball, R.J. Donahoe and D. Whittemore, (1989), *Groundwater geochemistry and water-rock interactions at Stripa*. Geochimica et Cosmochimica Acta 53, 1727–1740.

Pitkänen, P. and S. Partamies, (2007), *Origin and implications of dissolved gases in groundwater at Olkiluoto*. Posiva Oy, Eurajoki, Finland. Posiva Report 2007-04,57 p.

Pitkänen, P., A. Luukkonen, P. Ruotsalainen, H. Leino-Forsman and U. Vuorinen, (1998), *Geochemical modelling of groundwater evolution and residence time at the Kivetty site.* Posiva Oy, Helsinki, Finland. Posiva Report 98-07, 139 p.

Pitkänen, P., A. Luukkonen, P. Ruotsalainen, H. Leino-Forsman and U. Vuorinen, (1999), *Geochemical modelling of groundwater evolution and residence time at the Olkiluoto site*. Posiva Oy, Helsinki, Finland. Posiva Report 98-10, 184 p

Pitkänen, P., A .Luukkonen, P. Ruotsalainen, H. Leino-Forsman and U. Vuorinen, (2001), *Geochemical modelling of groundwater evolution and residence time at the Hästholmen site.* Posiva Oy, Eurajoki, Finland. Posiva Report 2001-01, 175 p.

Pitkänen, P., S. Partamies and A. Luukkonen, (2004), *Hydrogeochemical interpretation of baseline groundwater conditions at the Olkiluoto site*. Posiva Oy, Eurajoki, Finland. Posiva Report 2003-07, 159 p.

Puigdomenech, I. (ed.), I. Gurban, M. Laaksoharju, A. Luukkonen, J. Löfman, P. Pitkänen, I. Rhén, P. Ruotsalainen, J. Smellie, M. Snellman, U. Svensson, E-L. Tullborg, B. Wallin, U. Vuorinen and P. Wikberg, (2001), *Hydrogeochemical stability of groundwaters surrounding a spent fuel repository in a 100,000 year perspective*. Posiva Oy, Report POSIVA 2001-06, 84 p.

Raiswell, R. and D.E. Canfield, (1996), *Rates of reaction between silicate iron and dissolved sulphide in Peru Margin sediments*. Geochimica et Cosmochimica Acta 60, 2777-2787.

Smellie, J.A.T., R. Blomqvist, S.K. Frape, P.Pitkänen, T. Ruskeeniemi, J. Suksi, J. Casanova, M.J. Gimeno and J. Kaija, (2002), *Palaeohydrogeological implications for long-term hydrochemical stability at Palmottu*. Luxembourg, European Communities, Nuclear science and technology, EUR 19118 en, 201-207.

Vieno, T. and H. Nordman, (1999), *Safety assessment of spent fuel disposal in Hästholmen, Kivetty, Olkiluoto and Romuvaara – TILA-99*. Posiva Oy, Helsinki, Finland. Posiva Report 99-07, 253 p.

UNDERSTANDING SHIELD GROUNDWATER FLOW DOMAIN EVOLUTION DURING THE QUATERNARY PERIOD TO BUILD CONFIDENCE IN REPOSITORY LONG-TERM SAFETY

M. Ben Belfadhel, M. Jensen
Nuclear Waste Management organization, Canada

Abstract

The Nuclear Waste Management Organization (NWMO) is responsible for implementing Adaptive Phased Management, the approach selected by the Government of Canada for long-term management of nuclear fuel waste generated by Canadian nuclear reactors. In support of this objective, NWMO is pursuing an active technical research and development programme in collaboration with Canadian universities, consultants and international waste management organizations. A key objective of the geoscience component of the programme is to assemble geoscientific evidence to advance the understanding of deep-seated groundwater flow system evolution within typical Canadian Shield settings at time scales relevant to repository safety. This is achieved through a multidisciplinary approach where multiple lines of reasoning are used to gain insight in the processes and mechanisms affecting the long-term Shield flow system stability and its resilience to external perturbations. Specific issues that are being considered include the influence of flow perturbations by long-term climate change (temporal and spatial surface boundaries), oxygenated glacial melt water recharge, fracture network characteristics, variable saline flow domains and permafrost generation and decay. This paper provides an overview of selected programme activities that are intended to improve the understanding of Shield flow evolution.

Introduction

The Nuclear Waste Management Organization was established by the nuclear electricity generators in Canada and is responsible for implementing Adaptive Phased Management (NWMO, 2005), the approach selected by the Government of Canada for long-term management of nuclear fuel waste generated by Canadian nuclear reactors. In support of this objective, NWMO is pursuing an active technical research and development programme in the area of used fuel storage and repository engineering, geoscience, safety assessment, and technical support to the development of a collaborative siting process (Russell *et al.*, 2007).

The geoscience component of the technical research programme is designed to develop a geoscientific basis for understanding long-term geosphere barrier performance and build confidence in deep geological repository safety for both crystalline and sedimentary settings (Jensen, 2005). This is achieved by using a multidisciplinary approach involving the co-ordinated efforts of 20 research groups drawn from Canadian universities, consultants, federal organisations and international research institutions. Specific geoscience areas being considered include geology, structural geology, remote sensing, geostatistics, hydrogeochemistry, isotope hydrogeology, hydrogeology, paleohydrogeology,

natural analogues, numerical methods, seismicity, long-term climate change (i.e. glaciation) and geoscientific visualisation. The main objectives of the work programme include:

- develop field and laboratory techniques to improve site characterization capabilities in order to develop integrated conceptual site descriptive models;
- advance the understanding of long-term physical and geochemical stability of deep groundwater flow systems in fractured porous media at time scales relevant to repository long-term safety;
- improve numerical methods to assess the geosphere long-term evolution and its response to external perturbations, and to explore and constrain spatial and temporal uncertainties arising from limitations of site characterization; and
- develop visualization tools for integrating, archiving and communicating geoscientific information.

The approach is to place particular emphasis on integration and coordination of the various multidisciplinary work programmes to improve clarity and transparency of the geoscience evidence and logic that supports the development and demonstration of site-specific conceptual geosphere models. This process provides a systematic framework for testing hypotheses and geosphere response to relevant events and processes that affect long-term far-field stability. It also provides a forum for consensus building amongst multidisciplinary groups to understand how their respective contributions influence the overall confidence in the descriptive models and predictive model outcomes. Emphasis is also placed on the use of multiple lines of reasoning to constrain both the geosphere descriptive models and predictive numerical realizations for flow and mass transport.

As part of this approach, efforts have been focused on developing illustrative case studies of deep Shield groundwater flow system evolution at time frames relevant for long-term radioactive waste deep geological repositories. Selected programme activities being carried out to support the development of these illustrative studies are discussed in the following sections.

Canadian shield groundwater flow system evolution studies

As mentioned above, one specific objective of the geoscience work programme is to assemble geoscientific evidence to advance the understanding of groundwater flow system evolution and dynamics within deep-seated regional and local scale Shield settings. A multidisciplinary approach is used to assess the processes and mechanisms contributing to an understanding of long-term flow system stability and its resilience to external perturbations (Jensen and Goodwin, 2003). Specific issues that are being considered include the influence of flow perturbations by long-term climate change (temporal and spatial surface boundaries), oxygenated glacial melt water recharge, fracture network characteristics, permafrost generation and decay and variable saline flow domains (Jensen, 2005). The geoscience work programme also involves developing geoscientific visualisation tools to support the integration, validation and communication of complex and numerical modelling results and site characterization data.

Regional and sub-regional shield flow system analyses

Numerical models have been developed at both regional and sub-regional scales to advance the prediction of groundwater flow and mass transport in fractured crystalline Shield settings (Sykes *et al*., 2003, 2004 and 2005). Such numerical models serve as a systematic framework to assemble and test conceptual site descriptive models; develop methodologies to assess the influence of site

characterisation uncertainty on numerical groundwater flow and transport predictions and to improve the utility of numerical codes to enable a more rigorous assessment of flow domain uncertainty.

The regional flow system analyses were performed to examine and illustrate the evolution and distribution of current physical and chemical Shield flow system properties on regional groundwater characteristics and the influence on long-term climate change, particularly, time-dependent hydraulic, mechanical and temperature boundary conditions on flow system evolution. Specific aspects that were considered include: variable groundwater salinity distributions, spatially variable permeability fields, assumed flow system dimensionality; and residual glacial over-pressures on flow paths, flow rates and residence time. The regional scale analyses were performed using a three-dimensional numerical model of a hypothetical 5 734 km^2 watershed situated on the Canadian Shield (Figure 1). The model was based on a realistic and accurate description of the complex topography and surface water network characteristics. Parameters and characteristics used in the model were derived, in part, from data gathered at the Whisteshell Area in Southeastern Manitoba, Canada, and from other crystalline rock settings in Finland and Sweden (Sykes, 2005).

The regional numerical analyses provided insight into Shield flow systems, which may still be in a transient state as a consequence of the retreat of the Laurentide ice-sheet that covered the Canadian Shield during the last glacial episode. The results indicated that because of the complex topography and a rock permeability that decreases with depth, the flow that occurs in deeper rock represents a very small fraction of the total water budget in the watershed as the water balance is dominated by shallow flow with relatively short flow paths. The flow system dimensionality coupled with salinity and permeability distributions creates a deep-seated sluggish flow system in which solute transport maybe diffusion dominated (Sykes *et al.*, 2003).

Figure 1. **Regional scale domain showing surface water features and selected sub-regional domains (Sykes *et al.*, 2005)**

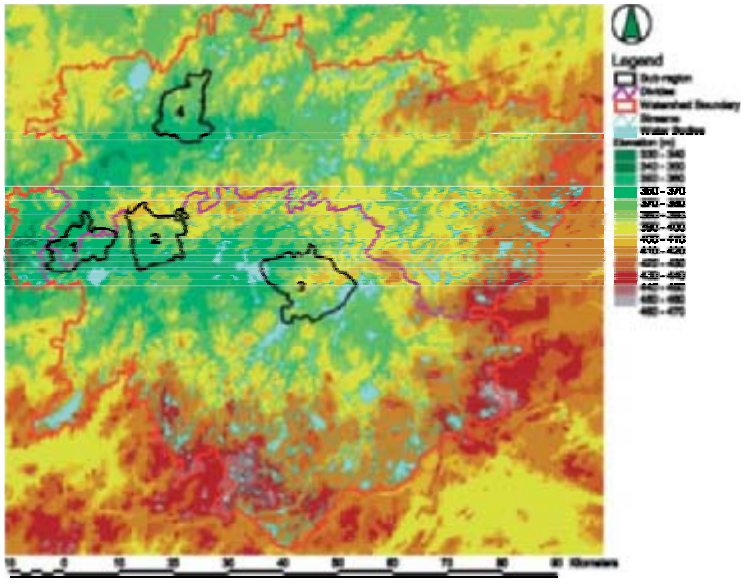

The sub-regional flow system simulations were performed on an 84 km^2 portion of the regional Shield watershed at a much higher numerical resolution (Sykes *et al.*, 2004). The model applied was a hybrid, discrete-fracture, dual continuum realization of the finite element code FRAC3DVS. The model was developed to assess the behaviour of Shield flow domains containing complex three dimensional curvilinear fracture networks and to illustrate whether the flow system at repository depth

remains stagnant and diffusion-dominated regardless of the uncertainty in fracture zone geometry and interconnectivity. The modelling approach included use of a realistic complex Fracture Network Model (FNM) that honoured many of the site-specific geological, statistical, and geomechanical constraints (Srivastava, 2002a, 2002b, 2003, 2005). A number of modelling scenarios were considered in order to examine the influence of uncertainties inherent to site characterisation including: the use of 100 equally probable FNM realizations, each constrained to measured surface lineaments; variable groundwater salinity; spatially-correlated depth-dependent permeability fields in the fracture zones and rock matrix continua and variable fracture zone width and porosity. An example of depth-dependent fracture zone distribution for sub-regional flow domain is illustrated in Figure 2.

Further activities related to improving the utility of numerical predictive tools have involved the implementation of a time domain probability technique within FRAC3DVS. This technique involves the solution of the advective-dispersion equation to derive Probability Density Functions (PDFs) that represent the statistical occurrence of water particles with time as a consequence of mixing processes. Such PDFs can be representative of "life expectancy" (time to discharge) or groundwater age (time since recharge). The analyses performed using the sub-regional model indicate that the Mean Life Expectancy (MLE) can be a useful performance measure in assessing the influence of the uncertain characteristics that may affect the long-term safety of a deep geological repository in a fractured crystalline rock setting in the Canadian Shield. Mean Life Expectancy represents the average travel time for any subsurface particle to discharge to the biosphere, while honouring both advective and diffusive dispersion processes, unlike particle tracking which can only honour advection. Since MLE is characterized by a probability density function, its mean may not represent earliest arrival, and hence, must be used with caution. Figure 3 shows distribution of MLE for four horizontal slices at different elevations. The figure shows that at an elevation of -300 m (600-800 m below ground), Mean Life Expectancy becomes greater than 10^6 years for most areas except within major fracture zones.

Figure 2. **Example of depth-dependent fracture zone permeability distribution (median trend) for sub-regional flow domain**

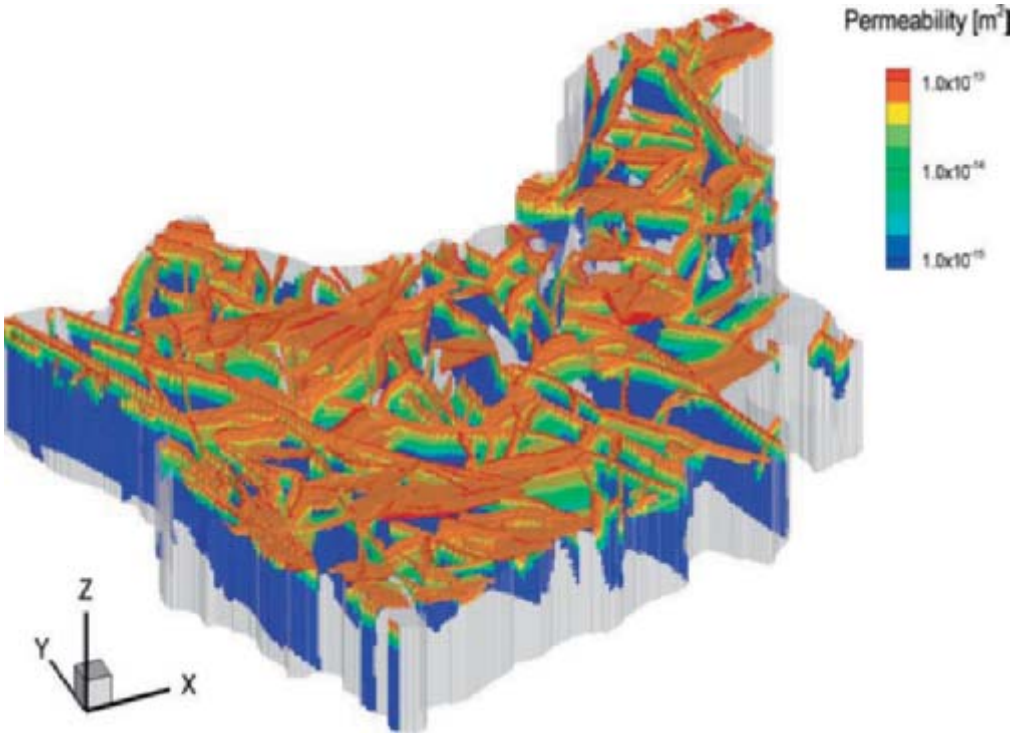

The MLE concept was used to assess the impact of fracture zone permeability, width and porosity on travel time. Permeability appears to exert the most significant influence, followed by width and porosity. Preliminary results show that decreasing fracture zone permeability can increase the travel time by several orders of magnitudes. The fracture zone permeability observed at shallow depths can significantly overestimate the risk associated with a deep repository if it is used for fracture zones at depth. The influence of fracture zone porosity on travel time in the sub-regional model is minimal compared to the effects of fracture zone permeability since the fluid volume in the rock matrix is much larger than in the fracture zones. Fracture zone width is, in general, an important factor for travel time distribution within the flow domain as it may increase or decrease transmissivity. However, it has a small impact on typical Canadian Shield settings where fracture zone width was observed to vary within one order of magnitude. The presence of brines at depth was shown to reduce the topographic gradient by requiring a greater energy potential to displace them. As deep pore fluid concentration increases, the shallow zone accommodates higher fluxes, while fluxes at depth decrease.

Long-term climate change – Glaciation

Glaciation/deglaciation is likely the most intense of plausible natural perturbations to the sub-surface hydrogeological regime. Given that the North American continent has been re-glaciated approximately every 100 000 years over the past million years, it is strongly expected that a deep geological repository within the northern latitudes in the crystalline rock of the Canadian Shield will be subject to glaciation events associated with long-term climate change.

As surface conditions are predicted to change from present day boreal to periglacial then followed by variable ice-sheet thickness cover and then rapid glacial retreat, transient geochemical, hydraulic, mechanical and temperature conditions will be simultaneously imposed on the Shield flow system. Geoscience research activities related to glaciation events and their impacts on the Shield flow system evolution are being undertaken using a multidisciplinary approach aimed at collecting multiple lines of evidence drawn from coupled numerical simulations, geochemical studies and paleo-hydrogeological investigations. The main aspects being considered include:

- expected Shield physical and temporal surface boundary conditions related to potential future glaciation events by estimating the magnitude and time rate of change of ice sheet thickness, ground surface temperature and permafrost occurrence, amongst other attributes;
- impacts of Coupled Thermo-Hydro-Mechanical effects imposed by glacial cycles on groundwater flow system dynamics;
- impacts of climate change on redox stability using both numerical simulations and paleohydrogeological investigations; and
- permafrost evolution and its role in influencing flow system evolution and fluid movement in Shield terrain using field investigations.

Understanding the response of the geosphere to glaciation events provides insight in past resilience of the geosphere at repository depth, which could enhance confidence in its future stability in the safety case for deep geological repositories.

Figure 3. **Mean lifetime expectancy at four different elevations in the sub-region**

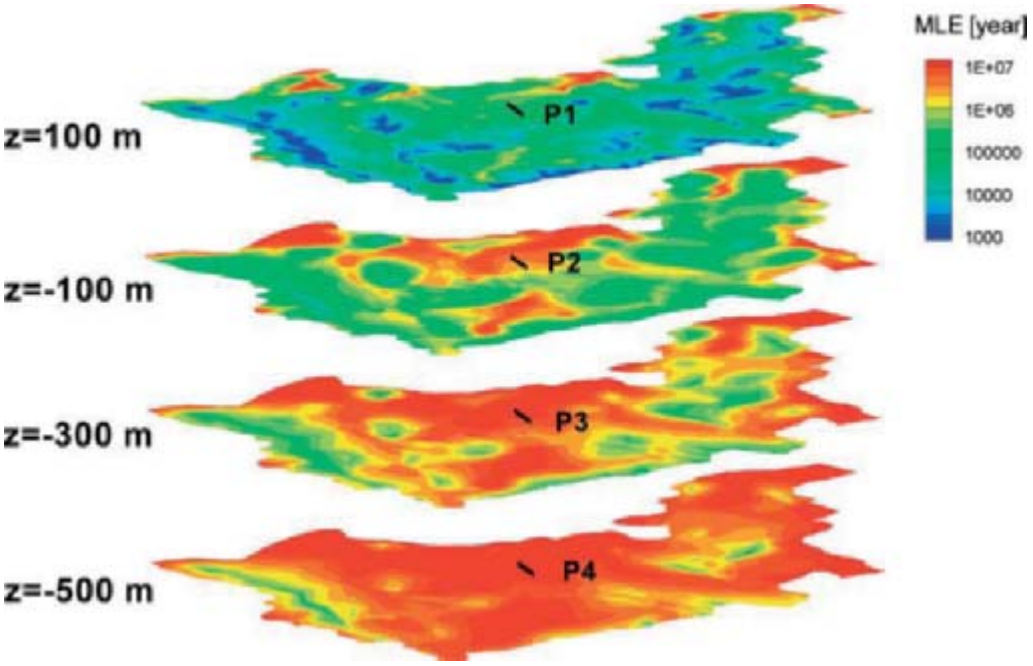

Evolution of Shield Surface Boundary Conditions during Glaciation cycles

In order to provide a detailed understanding of expected surface boundary conditions that would prevail during a future glaciation-deglaciation event, a series of simulations of the last Laurentide (North American) glacial cycle have been undertaken using the University of Toronto Glacial System Model, GSM, (Peltier, 2003, 2005, 2006a; 2006b).

The purpose of these simulations is to yield constrained predictions of the magnitude, duration and time rate of change of peri-glacial, glacial and boreal regimes that have perturbed Shield flow domains in the geologic past. Specific features that the model yields include ice-sheet geometry, advance and retreat, ground surface temperatures, basal ice-sheet meltwater fluxes, glacial isostatic depressions, and permafrost evolution. The GSM model uses a wide range of geophysical, geological and geodetic data, such as sea level histories, ice margin position, and present day rates of rebound to constrain the calculations and evaluate the degree of non-uniqueness in predicted ice-sheet histories and ground surface temperatures. An example of the complex and dynamic nature of surface and permafrost conditions reasonably expected to influence a hypothetical Shield site is shown in Figure 4.

Working with the Glacial System Model and efforts to provide explicit linkage to numerical analyses of sub-surface hydrogeology are yielding a new understanding of groundwater flow system evolution and response to glacial perturbations. This understanding not only provides a reasoned basis to examine issues of geosphere stability, but offers an improved basis for the integrated interpretation of geoscientific data necessary for developing a coherent descriptive geosphere model.

Figure 4. **University of Toronto Glacial Systems Model - prediction of Laurentide ice-sheet and permafrost evolution at a representative Canadian Shield site (Jensen, 2005)**

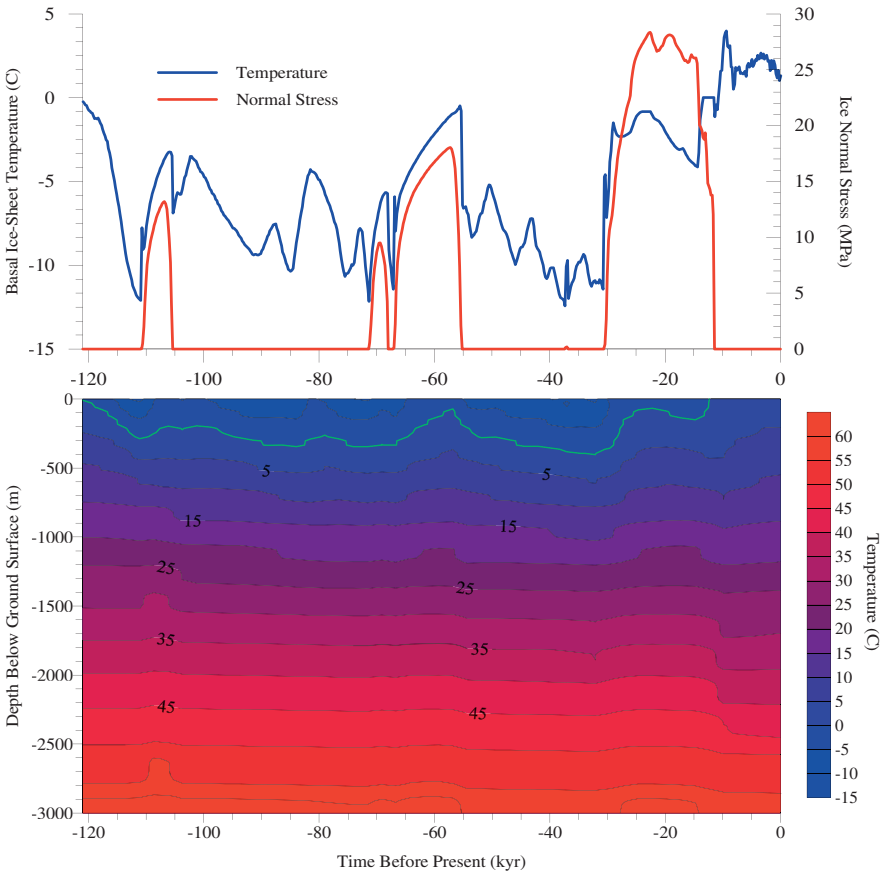

Thermo-hydro-mechanical effects associated with glaciation

Geoscience activities in this area are being conducted through Canada's participation in Task E of the international DECOVALEX III project, Development of Coupled models and their Validation against Experiments in waste isolation, (Chan *et al.*, 2006). The objective is to examine Thermo-Hydro-Mechanical (THM) effects of a glacial event on groundwater flow system dynamics at time scales relevant to repository performance (about 100 000 years) and provide a reasoned basis to support the treatment of long-term climate change in Performance Assessment and to assemble the overall repository safety case.

The main aspects that are currently being explored in Task E include: the magnitude and rate of change of hydraulic heads, gradients and groundwater fluxes; depth of penetration of glacial meltwater; and the influence of salinity and fracture zone orientation and interconnectivity on groundwater movement during a glacial event. The numerical simulations are performed using the MOTIF finite element code and 3-D and 2-D site-specific conceptual geosphere models adapted from the sub-regional scale flow system model describe earlier. The MOTIF modelling domain was based on the digital surface elevation map, the surface hydrology and a reduced version of the fractured network considered in the sub-regional flow model. Transient glacial loading/unloading boundary conditions were obtained from the University of Toronto Glacial System Model for a 120 000-year Laurentide glaciation scenario including transient normal stress and temperature conditions and basal

ice-sheet meltwater production rates. Some highlights of the preliminary results obtained for the specific conditions modelled include:

- the hydro-mechanical coupling associated with glacial loading increases the subsurface hydraulic heads by approximately 1/3 of the basal normal stress applied by the ice sheet;
- sensitivity analyses showed that a temperate glacier, very low permeability rock (~ 10^{-20} m^2) and less well connected fractures are necessary for residual hydraulic heads to persist at depth for thousands of years following ice-sheet retreat;
- adding thermal coupling to the Hydro-Mechanical (HM) simulations generally increases groundwater velocity by reducing water viscosity, while including salinity effects generally decreases groundwater velocity by increasing water viscosity and density;
- for the simplified version of the fractures network considered in the model, fracture zone orientation and interconnectivity were not found to greatly affect predicted groundwater velocity, perhaps as a consequence of the assumed high permeability in the modelled fracture zone as well as in the upper rock mass regions.

An important aspect with respect to the effect of glaciation on groundwater flow system and repository safety is whether altered boundary conditions could potentially create a situation for oxygenated recharge to reach typical repository depth. Advective particle tracking using constant fracture zone permeability with depth and without considering the influence of salinity suggests glacial meltwater recharge depths of one to several hundreds of metres via long connected fracture zones. However, simulations conducted taking into account depth-dependent salinity leads to shallower recharge of glacial meltwater. The influence of glacial meltwater recharge on redox stability is discussed in the next section.

Impact of climate change on redox stability

The influence of future climate change and altered physical and chemical boundary conditions on the stability of redox conditions is an important issue that the technical research programme is looking at using two complementary approaches. One approach involves the application of numerical models to simulate the long-term evolution of hydrogeochemical conditions in fractured crystalline rock. The other investigates the presence or absence of weathering signatures in minerals adjacent to fractures in crystalline rock, to provide information on the maximum depth of penetration of oxygen carried by recharging groundwaters in the past.

Numerical simulations using reactive transport modelling were applied to: provide a greater understanding of redox processes under simplifying assumption of oxygenated recharge water to depth of 500 m in fractured crystalline rock; identify the most important parameters controlling oxygen ingress; and demonstrate the capabilities of multicomponent reactive transport models in fractured crystalline rock (Spiessl *et al.*, 2006). Modelling scenarios considered included hypothetical glacial meltwater recharge into both a single fracture and fracture zone. These scenarios were, to the extent possible, constrained using parameters values characteristic of Canadian Shield rock. In the single fracture-matrix system, oxygen diffusion into the rock matrix and oxygen consumption by reduced iron minerals such as biotite was found to limit the depth of dissolved oxygen migration into the reducing region of the host rock to less than 15 m during a simulated melt water production of 10 000 years. For the fractured zone case, which is characterized by a larger oxygen-mass loading, the ingress of oxygen into the reducing zone was limited to depths of about 70 m (Figure 5).

Figure 5. **pO2 distribution with time and depth in a fracture (a) and in the fracture zone (b)**

a) Single Fracture

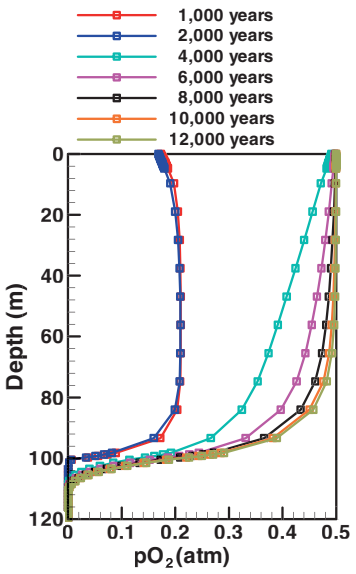

b) Fracture zone

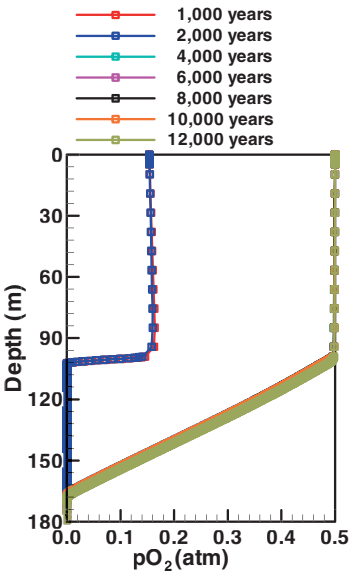

Uncertainty analyses demonstrated that for the set of parameters investigated, the most influential on oxygen migration for the single fracture-matrix case are: flow velocity in individual fractures, fractures aperture, biotite reaction rate in the rock matrix, the partial pressure of oxygen in the recharge water in the fracture zone, and the volume fraction of chlorite in the fracture zone.

Paleohydrogeological studies have been conducted at the Whiteshell Research Area in South-eastern Manitoba (WRA), Canada, to investigate past weathering events in crystalline rock. If evidence was found that fractures in crystalline rock provided pathways for the ingress of oxygenated waters to repository depths (500–1 000 m) in the past, there would be concerns that similar conditions may develop in the future. Previous studies (McMurray and Ejeckam, 2002; Gascoyne *et al.*, 2004), which used optical microscopy, electron microprobe analyses and isotope geochemistry, found that evidence of low-temperature oxidative weathering was limited to depths of less than 20 m.

More recent studies (Cavé and Al, 2005, 2006) used higher resolution techniques such as Transmission Electron Microscopy (TEM) to examine samples of drill core sections from the WRA adjacent to vertical fractures at depths between 7 and 240 m. Samples were also collected further away from the fractures to examine mineralogical features related to older, high-temperature alteration, to enable these features to be discriminated from low-temperature weathering patterns. The results of the analyses confirmed the conclusions of earlier studies and showed no evidence of low-temperature weathering at great depths. Very small amounts of biotite weathering products such as kaolinite, gibbsite and goethite were found in a fractured sample from 7 m depth. The only other evidence of low-temperature oxidation was found in samples below 7 m was a very thin Fe oxyhydroxide coating (40-100 nm thick) observed around pyrite in a sample from 65 m depth, at a distance of 20 mm from the vertical fracture (Figure 6)**.** Even at high magnification in the TEM, no oxyhydroxide coating was observed in other samples from greater depths. The results demonstrate that analytical TEM techniques can be effectively applied to find evidence of Fe mineral weathering in the form of very small oxidised phases that are not detectable by techniques with lower resolution.

Figure 6. **Iron oxyhydroxide along a boundary between chlorite and pyrite in specimen from 65 mm depth, and approximately 20 mm from a vertical fracture (Cavé and Al, 2006)**

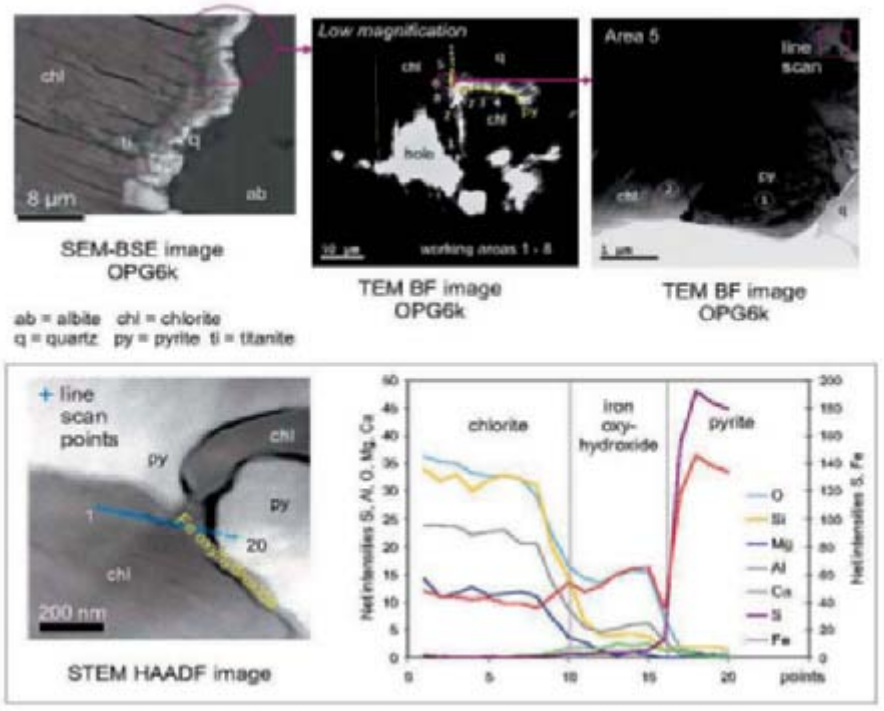

Imaging and analytical techniques: SEM = scanning electron microscopy. BSE = backscattered electron. (S)TEM = (scanning) transmission electron microscope. BF = bright field. HAADF = high angle annular dark field. EDS = energy dispersive X-ray spectroscopy.

Conclusion

The long-term evolution of the Canadian Shield groundwater flow system is a key research topic within the geoscience component of the NWMO technical research programme on used nuclear fuel. An integrated multidisciplinary approach and multiple lines of reasoning are being used to develop illustrative case studies to advance the understanding of deep-seated groundwater flow system evolution and its resilience to external perturbations. The focus is also on developing numerical tools and methods to improve the prediction of groundwater flow and mass transport in fractured crystalline Shield settings. These models provide a systematic framework to assemble and test conceptual site descriptive models, develop methodologies to assess the influence of site characterisation uncertainty on numerical predictions and improve the utility of numerical codes to enable a more rigorous assessment of flow domain uncertainty.

Regional and sub-regional groundwater flow analyses for typical Canadian Shield settings are providing evidence that the Shield flow domain at repository depths is characterised by stagnant groundwater flow systems where diffusion is the dominant mass transport mechanism. The concept of Mean Life Expectancy is a promising tool that could be used as a performance measure in identifying and assessing the relative importance of relevant geosphere processes and parameters that affect the long-term evolution of groundwater flow systems in fractured crystalline rock settings.

The prediction of Shield surface boundary conditions during glaciation cycles and their explicit consideration in hydrogeological numerical analyses are yielding improved understanding of

groundwater flow response to glacial perturbations. While the results of coupled Thermo-Hydro-Mechanical numerical analyses suggest glacial meltwater penetration to depths varying from one to several hundred meters, both paleohydrogeological studies and numerical simulation using reactive transport modelling for typical Canadian Shield conditions are providing evidence that dissolved oxygen migration into the reducing zone remains limited to depths less than 100 m.

As a general observation, the various field and numerical simulations being carried out are providing evidence that groundwater flow systems within typical Canadian Shield settings at repository depth are stable and unaffected by surface events.

References

Cavé, L.C. and T.A. Al, (2005), *Paleohydrogeology – development of analytical TEM methods for paleoredox investigations*, Ontario Power Generation, Nuclear Waste Management Division Report 06819-REP-01300-10099-R00, Toronto, Canada.

Cavé L.C. and T.A. Al. (2006), *Paleohydrogeology – analytical TEM investigation of mineral weathering in the Whiteshell Research Area*, Ontario Power Generation, Nuclear Waste Management Division Report 06819-REP-01200-10156-R00, Toronto, Canada.

Chan T., M.R. Jensen, F.W. Stanchell and A. Vorauer (2006), *Numerical modelling of subsurface coupled THM processes in a sub-regional-scale groundwater flow system in a Canadian Shield setting during a glacial event: I. Conceptual model development*. In Proc. GeoProc 2006: Advances on Coupled Thermo-Hydro-Mechanical-Chemical Processes in Geosystems and Engineering. (Editors, Weiya Xu, Xiaolong Tan and Shengqi Yang). Nanjing, China, May 22-25, 2006.

Jensen, M.R (2005), *The Deep Geological Repository Technology Program: Towards a geoscience basis for understanding repository safety*, OECD/NEA Proceedings Linkage of Geoscientific Arguments and Evidence in Supporting the Safety Case, Second AMIGO workshop, Toronto, Canada, 20-22 September 2005.

Jensen M.R. and M.R. Goodwin (2003), *Groundwater flow system stability in Shield settings a multidisciplinary approach*, Geological Disposal, OECD/NEA Proceedings Building Confidence Using Multiple Lines of Evidence, First AMIGO Workshop Proceedings, Yverdon-les-Bains, Switzerland, 3-5 June 2003

McMurry, J. and R.B. Ejeckam (2002), *Paleohydrogeological study of fracture mineralogy in the Whiteshell Research Area*, Ontario Power Generation, Nuclear Waste Management Division Report 06819-REP-01200-10082-R00, Toronto, Canada.

Gascoyne, M., J. McMurry and R. Ejeckam, (2004), *Paleohydrogeologic case study of the Whiteshell Research Area*, Ontario Power Generation, Nuclear Waste Management Division Report 06819-REP-01200-10121-R00, Toronto, Canada.

NWMO (2005), *Choosing a way forward, The future management of Canada's used nuclear fuel*, Nuclear Waste Management Organization (available at www.nwmo.ca), Toronto, Canada.

Peltier, W.R. (2003), *Long-term climate change – glaciation. Ontario Power Generation*, Nuclear Waste Management Division Report 06819-REP-01200-10113-R00, Toronto, Canada.

Peltier W.R. (2005), *Long-term climate change: the evolution of Shield surface boundary conditions*, OECD/NEA Proceedings Linkage of Geoscientific Arguments and Evidence in Supporting the Safety Case, Second AMIGO workshop, Toronto, Canada, 20-22 September 2005.

Peltier, W.R. (2006a), *Laurentide glaciation: boundary condition data set*, Ontario Power Generation, Nuclear Waste Management Division Report 06819-REP-01200-10154-R00 Toronto, Canada.

Peltier, W.R. (2006b), *Laurentide glaciation: simulation of sub-glacial hydrology*, Ontario Power Generation, Nuclear Waste Management Division Report 06819-REP-01200-10162-R00, Toronto, Canada.

Russell S., F. Garisto, P. Gierszewski, M. Hobbs, M. Jensen, T. Kempe, T. Lam, P. Maak, G. Simmons, A. Vorauer, K. Wei, (2007), *Technical Research and Development Program for long-term management of Canada used nuclear fuel-Annual report 2006*, Ontario Power generation report No: 06819-REP-01200-10163-R00, Toronto, Canada.

Spiessl S.M., K.U. Mayer and K.T.B. MacQuarrie (2006), *Reactive transport modelling in fractured rock – redox stability study*, Ontario Power Generation, Nuclear Waste Management Division Report 06819-REP-01200-10160-R00, Toronto, Canada.

Srivastava, R.M. (2002a), *Probabilistic discrete fracture network models for the Whiteshell research area, Prepared by FSS Canada*, Ontario Power Generation, Nuclear Waste Management Division Report 06819-REP-01200-10071-R00,Toronto, Canada.

Srivastava, R.M. (2002b), *The discrete fracture network model in the local scale flow system for the Third Case study*, Ontario Power Generation, Nuclear Waste Management Division Report 06819-REP-01300-10061-R00, Toronto, Canada.

Srivastava, R.M. (2003), *Probabilistic models of 3D fracture geometry*, Proceedings 4th Joint IAH/CGS Conference September 29-October 1, 2003, Winnipeg, Manitoba, Canada.

Srivastava, R.M. (2005), *Fracture network modelling: an integrated approach for realization of complex fracture network geometries*, OECD/NEA Proceedings Linkage of Geoscientific Arguments and Evidence in Supporting the Safety Case, Second AMIGO workshop, Toronto, Canada , 20-22 September 2005.

Sykes J.F., S.D. Normani and E.A. Sudicky (2003), *Modelling Strategy to assess long-term regional scale groundwater flow within a Canadian Shield setting*, Proceedings 4th Joint IAH/CGS Conference 29 September-1 October, 2003, Winnipeg, Manitoba, Canada.

Sykes J.F., S.D. Normani, E.A. Sudicky and R.G. McLaren (2004), *Sub-regional scale groundwater flow within an irregular discretely fractured Canadian Shield setting,* Ontario Power Generation, Nuclear Waste Management Division Report 06819-REP-01200-10133-R00, Toronto, Canada.

Sykes J.F., E.A. Sudicky, S.D. Normani, Y-J. Park, F. Cornaton and R.G. McLaren (2005), *The evolution of groundwater flow and mass transport in Canadian Shield domain: A methodology for numerical simulation*, OECD/NEA Proceedings Linkage of Geoscientific Arguments and Evidence in Supporting the Safety Case, Second AMIGO workshop, Toronto, Canada , 20-22 September 2005.

HYDRAULIC AND HYDROCHEMICAL RESPONSE TO SEISMIC EVENTS

T. Nohara
Japan Atomic Energy Agency, Japan

Introduction

Water level changes related to seismic events are well known in Japanese hot springs. Record from old document is a valuable source of information for investigations of the regularity of coseismic groundwater change. Co-seismic groundwater anomalies that accompanied the 1946 Nankaido earthquake have been previously reported [1]. Water levels in the wells at the Dogo Hot Spring fell 14 m and returned to the original level after three months. Similar phenomena were observed repeatedly in the same wells during the Nankai earthquakes related to oceanic movement along the Nankai trough during the Hakuho era (684 AD), during the Houei era (1707 AD), and during the Ansei era (1854 AD). The magnitude of water level decline is consistent with expansive volume strain due to fault activity at this point [1].

Waters from springs in the tunnels of the Kamaishi mine were analyzed before and after earthquakes, to establish if earthquakes influenced the groundwater chemistry. However, significant changes in groundwater chemistry were not observed. Only minor changes were observed in SO_4 and HCO_3 in four cases [2]. Although there is little information concerning changes in geochemistry of groundwater solely due to seismic activity, indications of potential for geochemical changes are recorded by chemical changes in the rock in and around faults. For example, the reported results from a drilling survey in the Nojima fault after the 1995 southern Hyogo earthquake [3] indicated remarkable alteration of fault rock at about 300 depth m. The alteration zone is a zone of cataclasis characterized by leaching of biotite minerals and alteration of feldspar to clay up to 50 m into the hanging wall (granite) adjacent to the active fault.

These papers show that some water level changes are within predictable limits based on volume strain accompany fault activity. The results of groundwater observations in the Kamaishi Mine [4] and the Tono Mine [5] indicate that changes of groundwater flow and of groundwater geochemistry accompanying fault activity are temporary and smaller than seasonal variations. The width of geochemical influence around active faults is considered to be several dozen metres [6].

It is thought that widespread influence to the geological environment is limited in these cases [6]. On the other hand, for enhanced reliability of a geological isolation system, knowledge of the cause of any groundwater change, regional influences and size and duration of the perturbation are important. As part of the development of predictability and for evaluating the effect of changes to groundwater flow accompanying future fault activity, factors assumed to control groundwater level changes need to be understand and considered for predictive modelling. Therefore the results of an assessment of existing information and a case study in the northern Awaji-shima, the western Tottori earthquake source region, and the Tono area are described in this paper.

Causes of groundwater level change

Information on proposed causes of water level changes during seismic events have been surveyed and studied. The observed distribution patterns of coseismic groundwater level changes are consistant with the expected distribution pattern of volumetric strain for a given focal mechanism [7,1,8,9]. In a confined aquifer, the coseismic water level changes correspond to volumetric strain [10]. The main aquifers near fault rocks, the high permeability fractured rocks, are often surrounded by lower permeability rocks around active faults [11]. Water pressure in this confined aquifer changes in response to crustal strain. The pressure records are similar to records of a broadband seismograph response to a distant earthquake [12]. Using long-term observations of groundwater level, Igarashi & Wakita [13] investigated the influence of atmospheric pressure, tides and precipitation to develop an understanding of aquifer characteristics. They presented a technique to distinguish the influence of the former from the influence of diastrophism on an aquifer.

From an examination of the relationship between coseismic changes of water level and volumetric strain, it was observed that some wells exhibited changes equivalent to the estimate based on volumetric strain while other wells exhibited non-equivalent changes in the same direction as the volumetric change and/or had incredibly high groundwater level change independent of the volumetric strain change [8,13,14,15]. The main reason for the latter is likely to be heterogeneity of geological structures [13]. Various models address heterogeneities in the rock mass at various scales (e.g. [16-20]).

Changes in groundwater level that accompanied fault activities were temporary in many cases, and recovered in several months to several years [1]. Dissipation of pore pressure [21], filling by minerals [3,22] and decline in porosity accompanying recovery of crustal stress [22] are suggested reasons for the recovery.

Groundwater change accompanying fault activity

During the southern Hyogo earthquake in 1995 (moment magnitude: Mw 6.8), movement occurred on the Nojima fault in northern Awaji-shima. In this area, the greatest portion of springwater is considered to originate as groundwater in granite. High fluoride ion concentration in springwater also has a granitic origin [23]. The main chemical compositions of springwater in this area are similar [24] (Figure 1). It was shown that the model of volumetric strain could not fully explain the changes in groundwater level [25]. Most of the notable coseismic changes of groundwater level occur within 100 km of respective epicenters [26]. Using accurate data on the depth of wells and of the observation points in those areas, changes of groundwater levels in shallow wells (< 30 m), were 5 m or less in more than 90 percent of the wells. The maximum change was an 18 m water level decline. Similarly, the range in deeper wells (> 30m) was only several decimetres or less [27]. Beyond the Awaji-shima area, remarkable coseismic water level changes were observed but they are sporadic and unevenly distributed. It is considered that the distribution reflects heterogeneity of geologic structures, such as presence of a tectonic line [28].

The result of this survey indicates that both new springs and increased yield occurred in lowlands, while large-scale water shortages occurred in highlands. Precipitation in the highlands, the recharge area, is the origin of springwater [29]. It is thought that the main cause of the change in hydrogeology of the wells is permeability increase accompanying fault activity [29-30]. It is thought that change of the regional groundwater flow to lowlands from highlands reflects heterogeneities of geologic structures, when the permeability of a continuous aquifer increases with fault movement. Coseismic increase of the permeability is estimated to be about 7 times [30].

The western Tottori earthquake in 2 000 (Mw 6.8) occurred in inland Japan. Geological and water level investigations indicated that small faults and water level dropping are unevenly distributed in the domain in which an increase in shearing stress is predicted by numerical analyses [5]. Increased shearing stress may be the cause of coseismic changes near active faults.

Change of the regional groundwater level accompanying distant earthquakes

In the Tono area, central Japan, remarkable changes were observed in groundwater levels and water pressures accompanying distant earthquakes, with a maximum epicenter distance of 1 300 km. It is pointed out that water level and water pressure observations differ according to changes in geology for every observation point in this area [31]. In the Tono area, the tendency for the groundwater level and water pressure to change is clearly related to the theoretical strain quantity as defined by Dobrovolsky *et al.* [32]. The specific value of strain (about 10-8), is the boundary for the appearance of coseismic change. Clear correlations do not occur between the amounts of coseismic change and values estimated by volumetric strain. The amounts of coseismic water level decline are several centimetres to decimetres (a maximum of 43cm), and the amount is larger than seasonal variations. These changes can be explained by special local permeability change. In addition, it is shown that coseismic changes had clearly reduced within one year following earthquake events [31].

This is an example which suggests coseismic change of the regional groundwater flow system in the Tono area. Coseismic rising of water level in discharge areas and coseismic dropping of water level in recharge areas are also observed [5].

Long-term influence

Research on the long-term influence on groundwater change associated with fault activity is a future subject for improvement in reliability of a geological isolation system. Coseismic changes in the Tono area are related to the theoretical strain quantity. It can also be said that groundwater changes due to the 1995 southern Hyogo earthquake and the 2000 western Tottori earthquake are also related to the theoretical strain quantity. Therefore, in attempting to improve the reliability of a geological isolation system, it is possible to initially target the volumetric strain accompanying fault activity and model the change of groundwater flow accompanying the strain. The maximum volume distortion was presumed from distribution of active faults in the central part of Japan, including the Tono area. In the Tono area, the largest known volumetric strain changes occurred near the Atera fault zone in the northeast part of the area. The model predicting change in groundwater conditions relevant to this is being developed. In crystalline rock, continuity of any high permeability zone in a hydrogeologic structure and the magnitude of permeability change and duration are the main areas of interest.

In addition, remarkable coseismic changes in the Tono area are observed in boreholes into the Tono uranium deposit. Although faulting and relatively high permeability fractured rocks occur in the Tono uranium deposit and coseismic changes occur, the deposit has remained relatively stable for some time, and there is no indication of remarkable remobilization of uranium for the past several hundred thousands years at least [33]. Moreover, rich lead-zinc deposits are present in proximity to the Atotsugawa fault zone. Preservation of these mineral deposits suggests that the effect of the groundwater change accompanying the fault activity is limited.

Conclusion

The results of the research on changes to groundwater flow accompanying fault activity are as follows.

- In many cases, changes of groundwater flow accompanying fault activity are small.
- There are many examples of water table recovery in about several months.
- Significant water level changes are observed to reoccur at specific locations.
- In a confined aquifer, groundwater level changes corresponding to volumetric strain were occurred in response to fault movement.
- Fault movement in the northern Awaji-shima area generated initially increasing permeability of the aquifer, and then water table decline in recharge areas and water table rising in discharge areas.

Subjects for future research

The changes of groundwater flow in the deep underground are not well known, especially in terms of changes in the regional hydrogeologic structure of active faults. In particular, understand of the influence of heterogeneities in geological structures on hydrogeological changes will also be required in crystalline rock areas. A quantitive examination of the influence of diastrophism on hydraulic conductivity, on the distribution of high-permeability zones, which can change easily and hydraulic gradient is a desired outcome of observation and investigation in the underground. Furthermore, it is important to understand the groundwater flow system and strain recovery. It will be a subject for improvement of the long-term safety of geological isolation with additional field surveying and numerical analysis in a mobile belt.

Figure 1. **Location map and chemical composition of spring water in the Awaji-shima area**

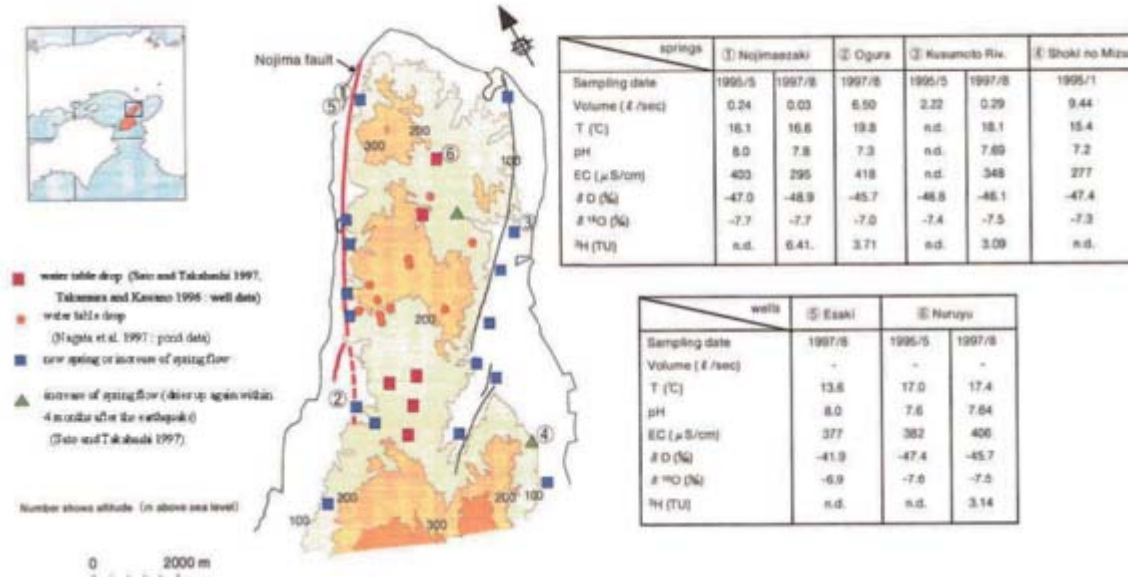

springs	① Nojimasaki		② Ogura	③ Kusumoto Riv.		④ Shoki no Mizu
Sampling date	1995/5	1997/8	1997/8	1995/5	1997/8	1995/1
Volume (ℓ /sec)	0.24	0.03	6.50	2.22	0.29	9.44
T (℃)	16.1	16.6	19.8	n.d.	18.1	15.4
pH	8.0	7.8	7.3	n.d.	7.69	7.2
EC (μS/cm)	403	295	418	n.d.	348	277
δ D (‰)	-47.0	-48.9	-45.7	-46.8	-46.1	-47.4
δ ^{18}O (‰)	-7.7	-7.7	-7.0	-7.4	-7.5	-7.3
^{3}H (TU)	n.d.	0.41.	3.71	n.d.	3.09	n.d.

wells	⑤ Esaki	⑥ Nuruyu	
Sampling date	1997/8	1995/5	1997/8
Volume (ℓ /sec)	-	-	-
T (℃)	13.6	17.0	17.4
pH	8.0	7.6	7.64
EC (μS/cm)	377	382	406
δ D (‰)	-41.9	-47.4	-45.7
δ ^{18}O (‰)	-6.9	-7.6	-7.5
^{3}H (TU)	n.d.	n.d.	3.14

References

[1] Kawabe I., (1991), *Groundwater accompanying an earthquake, a geochemical phenomenon*, Earthquake, 2, 44,341-364 (in Japanese with English abstract).

[2] Aoki, K., M. Kawamura, T. Ishimaru and H. Abe, (1999), *Survey and research of earthquake at Kamaishi mine*, Abstract of 1998 Annual Meeting of the Atomic Energy Society of Japan, p.788 (in Japanese).

[3] Tanaka H., T. Higuchi, S. Hinoki, K. Kosaka, A. Lin, K. Takemura, A. Murata and T. Miyata, (1998), *Deformation and alteration of fault rocks along the Ogura 500m core penetrating the Nojima Fault, Awaji Island, Southwest Japan*, Earth Monthly "The scientific drilling program of Nojima fault", No.21 special issue, pp.160-164 (in Japanese).

[4] Ishimaru, K. and I. Shimizu, (1997), *Groundwater pressure changes associated with earthquakes at the Kamaishi Mine, Japan -A study for stability of geological environment in Japan*, Proc. 30th Int. Geol. Congr., 24, pp.31-41.

[5] Japan Nuclear Cycle Development Institute, (2005), *H17: Development and management of the technical knowledge base for the geological disposal of HLW – Knowledge Management Report*- JNC TN 1400 2005-022.

[6] Japan Nuclear Cycle Development Institute, (1999), *H12: Project to Establish the Scientific and Technical Basis for HLW Disposal in Japan - Supporting Report 1 "Geological Environment in Japan"*, and JNC TN1400 99-021.

[7] Wakita H., (1975), *Water wells as possible indicators of tectonic strain*, Science, 189, 553-555.

[8] Koizumi N., (1994), *Crust strain and the fluid in the crust*, Volcanology, 39, 4,169-176.

[9] Matsumoto N. and N. Koizumi, (1998), *Change mechanism of the groundwater level as a quantity sensitivity diastrophism sensor*, Earth extra "new earthquake prediction research", 20,226-229 (in Japanese).

[10] Bredehoeft J.D., (1967), *Response of well-aquifer systems to Earth tides*, J. Geophys. Res., 72, 3075-3087.

[11] Nohara T., H. Tanaka K. Watanabe, N. Furukawa and A. Takami, (2006), *In situ hydraulic tests in the Active Fault Survey Tunnel, Kamioka Mine, excavated through the active Mozumi-Sukenobu fault zone and their hydrogeological significance*, Island Arc, Vol. 15, pp. 537-545.

[12] Kano Y. and T. Yanagidani, (2006), *Broadband hydroseismograms observed by close borehole wells in the Kamioka mine, central Japan: Response of pore pressure to 0.05 to 2 Hz seismic waves*, J. Geophys. Res., doi:10.1029/2005JB003656.

[13] Igarashi G. and H. Wakita, (1991), T*idal responses and Earthquake-related changes in the water level of deep wells*, J. Geophys. Res., 96, B3, 4269-4278.

[14] Roeloffs E.A. and E. Quilty, (1997), *Water level and Strain changes preceding and following the August 4, 1985 Kettleman Hills, California*, Earthquake, Pure and Applied Geophysics, Vol.149, pp.21-60.

[15] Roeloffs E.A., (1998), *Presistent water level changes in a well near Parkfield, California, due to local and distant earthquakes*, J. Geophys. Res., Vol.103, B1, pp.869-889.

[16] Sibson R.H., (1992), *Implication of fault-valve behaviour for rupture nucleation and recurrence,* Tectonophysics, 211, 283-293.

[17] Blampied M.L., D.A. Lockner and J.D. Byerlee, (1992), *An earthquake mechanism based on rapid sealing of faults*, Nature, 358, 574-576.

[18] Sleep N.H. and M.L. Blampied, (1992), *Creep, compaction and the weak rheology of major faults*, Nature, 359, 687-692.

[19] Rojstaczer S., S. Wolf and R. Michel, (1995), *Permeability enhancement in the shallow crust as a cause of earthquake-induced hydrological changes*, Nature, 373, 237-239.

[20] Brodsky E.E., E. Roeloffs, D. Woodcock, I. Gall and M. Manga, (2003), *A mechanism for sustained groundwater pressure changes induced by distant earthquakes*, J. Geophys. Res., Vol.108, No. B8, 2390, doi:10.1029/2002JB002321.

[21] Bosl W. & A. Nur, (1998), *Numerical Simulation of Postseismic Deformation due to Pore Fluid Diffusion, in Poromecanics*, Edited by J. -F. Thimus, Y. Abousleiman, A. H. -D. Cheng, O. Coussy, & E. Detournay, 23-28,Balkema, Rotterdam.

[22] Gratier J., P. Favreau and F. Renard, (2003), *Modeling fluid transfer along California faults when integrating pressure solution crack sealing and compaction processes*, J. Geophys. Res., 108, B2, 2104, ETG11-1, 11-25.

[23] Sato T. and M. Takahashi, (1995), *Groundwater change accompanying the southern 1995 Hyogo earthquake – Springwater produced in Awaji-shima*, the Coordinating Committee for Earthquake Prediction report, 54, and 732-734 (in Japanese).

[24] Sato T., M. Takahashi, N. Matsumoto and E. Tukuda, (1995), *Springwater of Awaji-shima produced after the southern 1995 Hyogo earthquake*, geology news, 496, 61-66 (in Japanese).

[25] Koizumi N., Y. Kano, Y. Kitagawa, T. Sato, M. Takahashi, S. Nishimura and R. Nishida (1996): *Groundwater anomalies associated with the 1995 Hyogo-Ken Nanbu Earthquake*, J. Phys. Earth, 44, 373-380.

[26] Sato T., M. Takahashi, N.Matsumoto and E. Tukuda, (1995), *Change (up to October, 1995) of groundwater accompanying the southern Hyogo earthquake*, environmental geology symposium collected papers, 5, and 41-44 (in Japanese).

[27] Ishimaru K., (1997), *Research regarding long-term stability of geological environment – Influence on the hydrology of groundwater by earthquake*, the Power Reactor and Nuclear Fuel Development Corporation Technical report, 102, 39-46 (in Japanese).

[28] Toda S., K. Tanaka, M. Chigira, K. Niyagawa and T. Hasegawa, (1995), C*oseismic groundwater action accompanying the southern 1995 Hyogo earthquake*, Earthquake, 2, 48,547-553 (in Japanes).

[29] Sato T., R. Sakai, H. Osawa, K. Furuya and T. Kodama, (1999), *Oxygen and hydrogen isotopic ratio of the groundwater which discharged unusually after the earthquake in Awaji-shima*, the Japanese Association of Hydrological Sciences, 29 and 1, 13-24 (in Japanese with English abstract).

[30] Sato T., R. Sakai, K. Furuya and T. Kodama, (2000), *The water head dispersion ratio presumed from the output change after an earthquake*, groundwater technology, 42 and 2, 16-22 (in Japanese with English abstract).

[31] King C.Y., S. Azuma, G. Igarashi, M. Ohno, H. Saito and H. Wakita, (1999), *Earthquake-related water-level changes at 16 closely clustered wells in Tono, central Japan*, J. Geophys. Res., 104, B6, 13,073-13,082.

[32] Dobrovolsky I.P., S.I. Zubkov and V.I. Miachkin, (1979), *Estimation of the size of earthquake preparation zone*, Pure and Applied Geophysics, 117, 1025-1044.

[33] Nohara T., Y. Ochiai, T.Seo and H. Yoshida, (1992), *Uranium-series Disequilibrium Studies in the Tono Uranium Deposit*, Japan, Radiochimica Acta, 58/59. 409-413.

TABLE OF CONTENTS

Session IV

Response and Resilience of Crystalline Rock to Natural Perturbations and Geosphere Evolution (buffering)

Poster Session